California AHMCT Center
University of California at Davis
California Department of Transportation

MACHINE VISION FOR AN AUTOMATED CRACK SEALING MACHINE

Kenneth R. Kirschke
Steven A. Velinsky

AHMCT Research Report
UCD-ARR-93-02-04-01

Iterim Report of Contract
SHRP-H-107A

February 4, 1993

* This work was supported by the California Department of Transportation (Caltrans) Advanced Highway Maintenance and Construction Technology Center at UC, Davis, by the Strategic Highway Research Program (SHRP), and by the United States National Research Council (NRC)

ACKNOWLEDGMENTS

Let us not forget the music by which we have sung. Thank you, Pamela, for providing most of the music.

Thank you, Dr. Velinsky for providing direction and encouragement through my graduate work. Additional thanks to my thesis committee, Dr. Ravani and Dr. Hsia for their time and helpful recommendations.

This work was supported by the Strategic Highway Research Program of the United States National Research Council and the California Department of Transportation through the Advanced Highway Maintenance and Construction Technology Research Center at the University of California at Davis, and this support is gratefully acknowledged.

ABSTRACT

Current methods for highway maintenance are both labor and cost intensive. In particular, the sealing of cracks costs the State of California over $10 million annually. A crack sealing team consists of approximately eight individuals that seal one to two lane miles per day. This translates to approximately $1800 per lane mile (1.6 km). Furthermore, the highway maintenance workers are exposed to the dangers of moving traffic. Meanwhile, the traffic becomes congested since lane closing is necessary during crack sealing.

Currently, research is underway at the Department of Mechanical Engineering of the University of California, Davis to design and develop a crack sealing machine that will sense, prepare and seal cracks in pavement. By developing this machine, the goals are to minimize the exposure of workers to the dangers of traffic, considerably increase the speed of operation, and improve the quality and consistency of the resultant seal. Improving the quality of the seal will result in extended time between major road rehabilitation. Furthermore, increasing the operation speed will reduce highway congestion due to lane closures.

The purpose of this thesis is to develop the Machine Vision System that will detect primarily the starting location of cracks in pavement surfaces for the Automated Crack Sealing Machine (ACSM). A local laser range finder based sensing system will be used to verify the presence of cracks that the machine vision system has identified. Additionally, the Local Sensing System will locate crack position and measure crack width to an accuracy such that the crack preparation, sealant application and shaping of the seal can be performed through machine automation. The local range sensor is under parallel

development and is included in another thesis effort by Krulewich (1992). A Machine Vision System using image acquisition and processing technology is developed and tested for crack detection requirements specific to the ACSM. Based on the tests performed, it is concluded that the Machine Vision System meets all crack detection requirements for a typical crack sealing operation in California; i.e., cracks of widths in the range 1/8 to 1 inch (3-25mm).

Table of Contents

List of Tables

List of Figures

CHAPTER 1 - INTRODUCTION

Worldwide, a tremendous amount of resources are expended annually maintaining highway pavement. Much of these expenditures involve the sealing of cracks, which when properly performed can help retain the structural integrity of the roadway and considerably extend the time before major rehabilitation is required. The sealing of cracks is a tedious, labor-intensive operation. Furthermore, the procedure is not standardized and there is a large distribution in the quality of the resultant seal. In addition, while crack sealing, the work team is exposed to a great deal of danger from moving traffic in adjacent lanes.

As such, a project has been underway to develop automated crack sealing machinery in order to:

- Minimize the exposure of workers to the dangers associated with working on a major highway.
- Considerably increase the speed of the operation.
- Improve the quality and consistency of the resultant seal.

Furthermore, increasing the speed of the operation will in turn reduce the accompanying traffic congestion since lane closure times will decrease.

In order to have the greatest impact, such machinery should satisfactorily perform the following functions automatically:

- Sense the occurrence and location of cracks in pavement.
- Adequately prepare the pavement surface for sealing with the appropriate methods; for example, any operation that is deemed necessary such as removing entrapped moisture and debris, preheating the road to ensure maximum sealant adhesion, refacing of reservoirs, etc.
- Prepare the sealant for application; i.e., heat and mix the material, etc.
- Dispense the sealant.
- Form the sealant into the desired configuration.

Additionally, the machinery will have many other more detailed overall functional specifications related to safety, cost, reliability, etc.

Clearly, a major aspect of the machinery to be developed concerns the automatic sensing and locating of cracks in pavement. There have been a number of studies that discuss automated pavement crack detection for purposes of categorizing pavement distress, and planning future maintenance activities (i.e., pavement management); see e.g., Bomar, et al. (1988); Butler (1989); Fukuhara, et al. (1990); Haas, et al. (1984,1985); Humplick & MacNeil (1988); Mahler (1985,1990); Maser, et al. (1985,1990); Ritchie (1990). Concerning crack sensing for automated pavement repair, Haas and Hendrickson (1990) have presented an algorithm for locating cracks that have been previously routed, and this algorithm has been demonstrated on a simulated roadway surface. Their algorithm has the potential to be quite useful for the pavement operations that they have concentrated upon, those being crack filling, patching, and spall repair.

As noted above, several recent studies have applied digital image processing to the recognition of cracks in highway pavement in the interest of classifying crack severity and extent as a basis for pavement management decisions. These "pavement-distress-survey" systems are expected to acquire data at a relatively high rate (e.g., on the order of 40 mph {64 km/hr}), as their primary purpose is to classify relatively large sections of highway. It is expected that maintenance workers would later be instructed as to the proper procedures for each section. Accordingly, such systems need to gather the following specific information (Mahler, 1990):

- *Number* of cracks,
- *Length* of each crack,
- *Direction* of each crack, and
- *Width* of each crack.

Furthermore, the positional accuracy required is relatively low as information is used primarily to identify the distress type of these sections with descriptions such as: alligator cracking, longitudinal cracking, potholes, etc. These systems are intended to detect cracks as small as one-sixteenth inch (1.6 mm) wide.

Crack sealing operations as they are performed manually, require high positional accuracy for a starting location of a crack segment, and a direction for efficient *tracing* of the crack with a sealant applicator and shaping tools. An automated crack sealing machine must demonstrate this functionality before it can perform any other function. This thesis develops the function of sensing the occurrence and location of cracks in pavement. A parallel thesis effort (Kruelwich, 1992) developed a local range sensor necessary to complement some of the limitations of the sensing system developed in this thesis.

A machine vision based algorithm for sensing and accurately locating unprepared cracks between one-eighth and one inch (3-25 mm) in width on Asphalt Concrete (AC) and Portland Cement (PCC) pavements has been successfully formulated and implemented. A crack sensing algorithm is necessary to automate existing crack sealing operations. The needs for automation include improvements in safety, quality, and efficiency.

In developing the function of crack sensing, the criteria for the sealing of transverse and longitudinal cracks in AC pavement are developed first. Secondly, specific requirements relating to automated crack sealing are developed for locating cracks. Thirdly, the requirements are used in surveying existing machine vision technologies and image processing efforts towards detecting pavement cracks. Finally, a technology is selected for crack sensing as part of the Automated Crack Sealing Machine (ACSM).

1.1 Criteria for the Sealing of Transverse Cracks in AC Pavement

The California Department of Transportation (Caltrans) has extensive experience at sealing cracks. As such, in order to gain a better understanding of the crack sealing process, crack sealing criteria were solicited from a Caltrans specialist[1]. Formal specifications were provided and used, in part, to develop the requirements of the machine vision. These specifications which are included in Appendix A, include criteria for the sealing of transverse and longitudinal cracks in AC pavement. Furthermore, these criteria are also relevant to the sealing of cracks in PCC pavement.

Cracking in AC pavement primarily occurs due to repeated thermal stresses, loss of binder in the asphalt over time, and overlaying of AC pavement on jointed PCC pavement (reflective cracking). The first significant cracks which occur usually span the entire road perpendicular to the road travel direction. This occurs due to the inability of the road to accommodate tensile stresses during its cyclical heating and cooling. It is the intention of sealing to prevent or prolong the type of damage that would require more extensive maintenance by identifying initial cracks and sealing them at the earliest possible time. A transverse crack caused by thermal cracking is sealed when it approaches 1/4 in (6 mm) in width. Since cracks are non-uniform in width, smaller crack widths are extensively present in cracks that approach 1/4 in (6 mm). The bulk of these smaller cracks are assumed by the researcher to be half of the maximum crack width or 1/8 in (3 mm).

The preparation of transverse cracks in AC pavement is extremely important to obtain adhesion between the pavement surface and the resultant seal. For good adhesion of recommended asphalt based sealant materials which

---

[1] Personal conversation with Mr. Ron Reese, Caltrans Crack Sealing Specialist, Office of Pavement, California Department of Transportation, 12/91.

are hot applied, the pavement to be sealed must be free of debris and moisture. Moisture removal is facilitated by preparing the pavement surface with the application of heat.

Although Caltrans recommends that the sealant material be squeegeed, dimensions regarding the sealant overband are not specified. These dimensions are important with respect to accuracy of the machine vision system and additionally ACSM end effector requirements. Information regarding the dimensions of a sealant overband are available through research conducted by the Utah Department of Transportation (Belangie, et al. 1985). This research led to the specification of squeegeeing in a "band-aid" configuration in Utah (see Fig. 1.1). Figure 1.1 shows that the maximum width of a seal for an 1/8 inch (3 mm) crack should be approximately 4.13 inches (10.5 cm). The minimum seal width is 2.13 inches (5.25 cm). If an apparatus applies the maximum width seal, then it can tolerate an error of 1 inch (25 mm) ([4.13-2.13]/2-sides) with respect to the centerline of the crack.

1.2 Criteria for the Sealing of Longitudinal Cracks in AC Pavement

Longitudinal cracks which require sealing (preventative maintenance) in AC pavement occur primarily due to reflective cracking from overlays on PCC pavements with longitudinal joints. Other "cracks" which warrant sealing are interface joints next to PCC pavement and cold joints next to AC pavement. If significant failure is occurring on an AC shoulder next to a PCC road bed, then a different level of maintenance would be required.

The preparation, sealants applied, and finishing characteristics are the same as for the sealing of transverse cracks in AC pavement. However, special mention needs to be made regarding AC/PCC interfaces. These joints, being out of the traveled way, usually contain a significant amount of debris and vegetation.

Some maintenance crews in California use pressurized water a day or two prior to the crack sealing operation in order to prepare longitudinal joints and cracks at such interfaces.

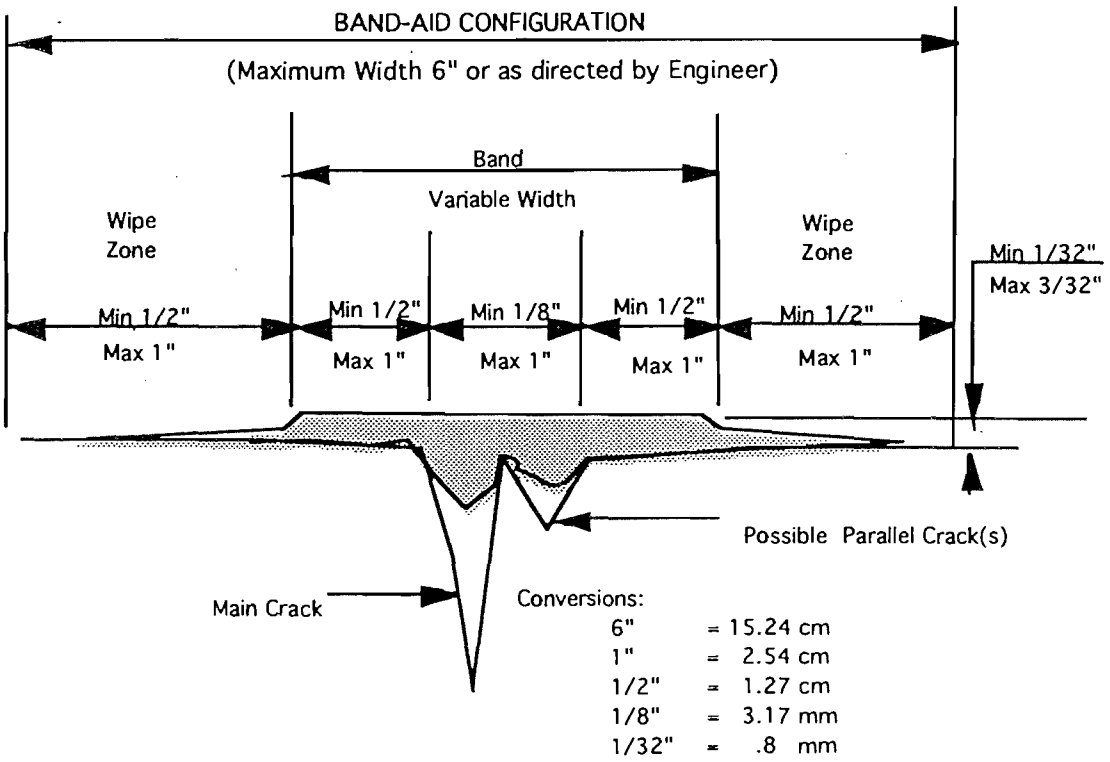

Figure 1.1 Squeegeed Seal Profile Recommended by Belangie, et. al.

1.3 Crack Sensing Requirements

In contrast to the requirements for *pavement-distress-survey* systems, automated crack sealing machinery must accurately locate individual crack segments so that they can be processed effectively. Additionally, through either the development of crack machine end-effectors (e.g., sealant dispensers and shapers) that are tolerant to variations in crack width or the use of the local sensing system, detailed crack *Width* data will not be required from the machine vision system provided it can identify all cracks that fall within the widths of concern. As such, of the four pieces of information required of a "pavement-

distress-survey" system, only *Length* and *Direction* information are required for the automated crack sealing machine. One additional piece of information is necessary, that being the starting *Location* of a given crack segment. Therefore, the following information, listed in order of importance, must be supplied by the vision system:

- *Location* of each crack segment,
- *Direction* of each crack segment, and
- *Length* of each crack segment.

Location is the most necessary information required to seal a crack. *Direction* information is useful, but with the appropriate path planning algorithms, this information could potentially be developed by the local range sensor provided the location could be obtained regarding the start of each crack segment. Finally, *Length* information would be useful for path planning, but for relatively predictable cracking (e.g., regularly occurring transverse cracking and joints), a local range sensor could identify the termination of the crack with minimal loss in efficiency. Length information would also be useful for omitting cracks that are not at least three feet in length, an informal criteria used in crack sealing practice. Therefore, the focus of the machine vision development effort and the measure of its success will be on its ability to find the starting *Location* of any given crack segment.

1.4 Technology Survey

Although previous work in pavement crack detection has employed image processing, other machine vision technologies may offer alternatives for automated pavement crack detection. In investigating alternatives for crack detection, functional criteria are developed and potential sensing technologies are investigated. The following sensor criteria are used in technology selection.

Sensor Criteria

Resolution:

The sensor will be able to resolve a roadway crack a minimum of 1/8 inch (3 mm) in width.

Accuracy

A crack will be recognized within 1 inch (2.5 cm) of crack edge location

Cycle Time:

The sensor system should be able to provide crack information continuously from a vehicle moving at a minimum speed of 2 mph (3.2 km/hr).

Type of interference and possible failure:

The sensor system should be resistant to the following:

- condensing moisture,
- acoustic noise,
- mechanical vibration and shock-3 g's peak vibration from 15 Hz to 100 Hz and 15g's non-operating for transport,
- heat (-20 to 160°F -29 to 71°C),
- dust and roadway debris (must be sufficiently strong to survive impacts from 3/8 in (9.5 mm) aggregate and roadway debris not exceeding 8 ounces (.23 kg),
- moisture on pavement,
- debris in cracks,
- road surface height variations,
- temperature variations,
- interference between adjacent detectors or between source and detectors,
- variations in lighting conditions, and

- electromagnetic interference from nearby machinery, such as a generator.

Reliability:

The sensor system and its expected maintenance should provide for a service life of 10 years.

Maintainability:

The system should be easily accessible for component replacement or adjustment. Also, components should make use of off-the-shelf technology.

The sensing technologies investigated for crack detection are shown in Fig. 1.2 and were completed in a previous effort (Jing et al., 1990). The most favorable prospects are shown in a striped background. Other potentially promising areas are shown with a dotted background. The highest level division for categorizing technologies for crack detection concerns the use of tactile or non-tactile sensing.

Tactile

A tactile sensor is one which recognizes a crack by being in direct contact with the pavement. A tactile sensor is thought to be the least desirable due to high amounts of wear associated with approximately 72 discrete sensing elements that would be required to cover 12 feet (3.66 m) of lane width. Two types of sensors are considered.

Microswitches are commercially available in many forms. The typical application usually involves the contacting of a smooth surface by a rolling element or a spring loaded by bending. The application to sensing cracks would involve the riding of the rolling element or the spring along the pavement. Based on the required crack resolution of 1/8 in (3 mm), a sensor of this type would

have trouble distinguishing between valleys among pieces of aggregate and true cracks. A sensor of this type would also have difficulty in sensing longitudinal cracks (parallel to the vehicle direction of travel).

TDR stands for Time Domain Reflectometry and is a method for sensing the dielectric constant of a material between electrodes. TDR is currently used by Caltrans to detect moisture under the pavement. TDR might be used for sensing cracks by allowing electrodes to ride along the pavement separated by a longitudinal and/or lateral distance of one to two inches. When a crack appears between electrodes, the change of dielectric from asphalt to asphalt and air would generate a spike.

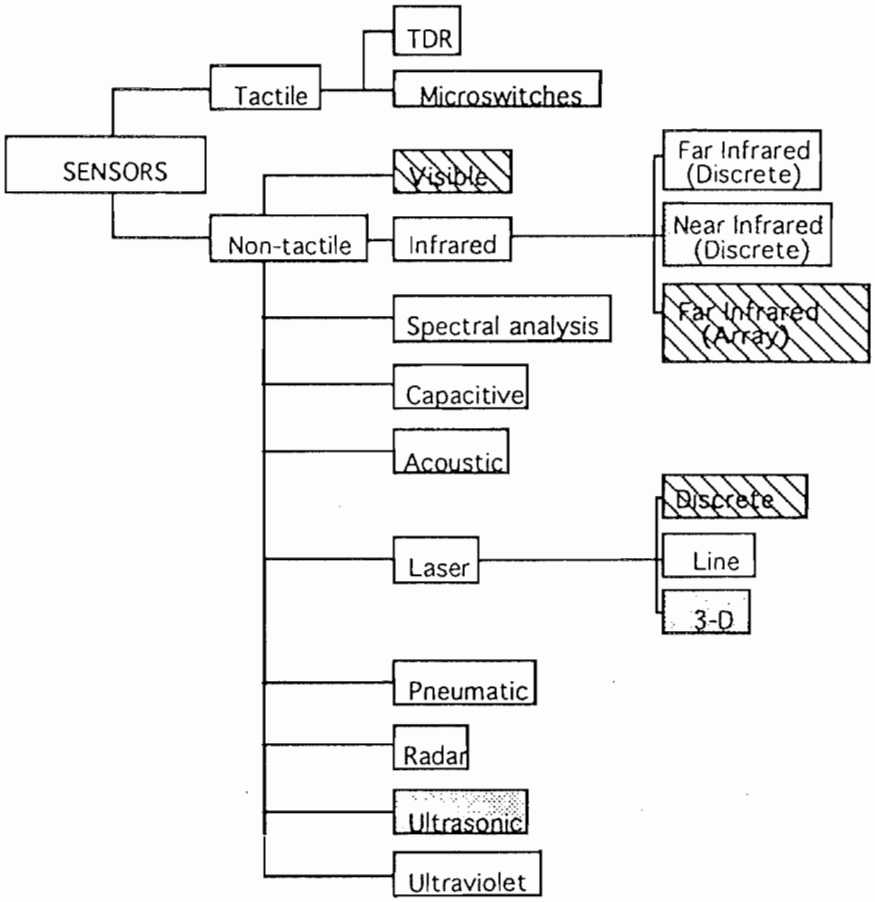

Figure 1.2
Technologies Investigated

This information could be manipulated to plot crack locations in x-y coordinates. Each electrode pair and TDR electrical hardware sells for around $7000. Several electrode pairs would be required and could be multiplexed and processed for crack detection using several sets of electrical hardware. Whether TDR would work in a "sliding along the surface" mode is not known. However, it would be difficult to maintain continuous surface contact on rough pavements and wear of the aluminum electrodes would be unfavorable.

Non-Tactile

A non-tactile sensor is one in which there is no physical contact with the pavement to establish the presence of a crack. This mode is thought to be the most desirable because it is associated with low amounts of wear. Several sensors are considered in this area.

Spectral Analysis is mentioned as a possibility due to the oxidizing which naturally occurs on the surface of AC pavement. Spectral analysis would involve looking for emission and absorption characteristics of the pavement surface. Oxidized pavement has less emissions that non-oxidized pavement. Since cracks are newly open to sunlight, their oxidation rate could be greater than the older surface. What would be required for this type of sensor would be a gun type "spectrascope". Currently, no commercial device exists of this type. The sensor developed of this type would most likely be a discrete sensor. Since these are not in production, the 72 or so (one for every 2 inches 5 cm of horizontal resolution) that may be required could be prohibitively expensive although it is not known how much it would cost to manufacture one of these units. There is also uncertainty as to whether this sort of a strategy would work.

Sound waves are not anticipated to provide the resolution or data acquisition rates required due to the relatively long wavelengths of sound and the limitations of the speed of sound in air.

Capacitive sensors are widely used in precision sensing of metallic objects in manufacturing environments. The sensor is itself one half of a capacitor and requires an object to be sensed to be a grounded conductor. Capacitive sensors are not possible for this application due to the non-conducting properties of asphalt.

Inductive sensors contain an oscillator which shows damping depending upon the material contained within the electromagnetic field of the sensor. They are not usable due to the shape of the field at the end of the sensor which does not provide enough resolution. The width of the field is usually about two times the sensing range. Therefore, in order to have 1/8 in (3 mm) resolution, a sensor would have to be 1/16 in (1.6 mm) from the pavement. Inductive sensors are primarily used for sensing the proximity of metal objects in highly structured environments.

Infrared sensors showed promise in the near and far infrared regions. Discrete far infrared sensors are thought of due to the anticipation that a crack would be evident by higher temperatures due to the radiation shape factor of the crack, or lower temperatures due to water intrusion. Initial experimentation with an infrared temperature gun showed that cracks are usually at a different temperature than surface pavement. Cracks in the direct sunlight showed hotter temperatures and shaded cracks or cracks with water intrusion showed cooler temperatures. The most positive results occurred when the pavement is preheated. This introduced a heat source to the cracks and the surface pavement. The surface pavement lost its heat rapidly leaving the crack at a temperature higher (1-5°F (.56-2.8°C)) than adjacent pavement. The response

time of an infrared temperature gun is slow and an attempt was made to use infrared sensing elements with amplifiers in order to get the desired response time that would be required for a discrete infrared sensor (300-600Hz). Two sensors are tried which utilized a heat sensitive plastic (PvdF) film as a sensing element with no success. When the plastic is heated, it creates a small voltage that is amplified. The effectiveness of the sensor is limited by the time it takes the plastic to respond to heat variations by expanding and contracting. The best response time is approximately 3 Hz which is far short of the required 300-600Hz response time.

Another area of far infrared sensors involves array sensors. The resolution can approach video resolution with the highest found to be 512x512 picture elements or "pixels". Of the different types of infrared cameras, there are vidicon tube based cameras and solid state based cameras without tube sensing elements. The tube element is least preferred due to the 1000 hour mean time between failure rates advertised. With the increased wear due to constant vibration on the road a solid state sensing element is preferable. A camera could be mounted above the roadway and grab a frame approximately three feet square (.9 m x .9 m). At two miles per hour (3.2 km/hr) the vehicle would travel this distance in 1 second which could be enough time for image processing hardware/software to process the image and generate a path for the sealant applicator to follow. Single operations over an image take approximately 1/30 of a second with PC based commercially available hardware. A far infrared camera would be expected to take advantage of the thermal properties of the pavement mentioned previously. At the time of the study, a solid state, far infrared camera runs about $95,000 and five would be required for a full lane width. Therefore, this method seems cost prohibitive and is not pursued further.

Near infrared sensors are looked at due to their prolific commercial use. These units are typically used to sense entrance into retail stores and to count presence and flow of materials in mass production environments. These units are discrete and are of the retroreflective type which create and receive their own signal. The rationale for using this sensor is that under normal operation, the sender and receiver are in view of one another through the reflection from the pavement. When a crack occurs this geometry is disturbed and the view is lost thus indicating a crack. However, this type of method is also just as sensitive to rises in pavement due to aggregate. In order to eliminate this effect a divider is placed between the sender and the receiver with the sender and receiver normally unaware of each other (see Fig. 1.3). In the presence of a crack, the increased distance provides the geometry necessary for receipt of the near infrared light source. If a rise in pavement occurs, the light source is still not visible just as it is in the presence of continuous pavement. This strategy could also be accomplished using fiber optic cable.

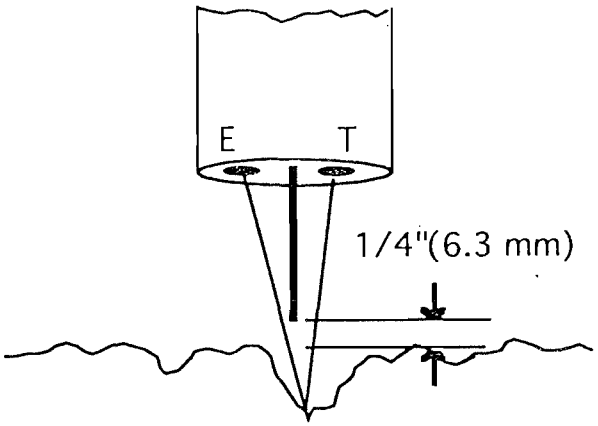

Figure 1.3
Near Infrared Sensor

Also, commercially available sensors have been found which incorporate a divider and a polarizer. The polarizer is an attempt to reduce reflection from light

colored objects in industrial applications such as labels on Aluminum soft drink cans. Reflection from light colored objects is also a problem on AC pavement. Light colored aggregate will give false readings with a divider due to the intensity of the light reflected from the white aggregate. The reflection is at such a high intensity that it gives false readings. A commercially available polarized unit used showed no improvement in sensitivity to light colored objects over the divider alone, therefore this approach is abandoned.

Laser range sensors operate in the near infrared region. They detect distances by the geometry of the reflecting beam. Typical units can have sensing ranges extending four inches (10 cm) from the sensor and terminating at a distance of eight inches (20 cm) from the sensor. It is usually designed to provide a linear output signal as a function of an object's distance within its range. The sensing head for these units costs approximately $1000 and the controller for the sensor costs approximately $1300. The only problem being that approximately 72 of these would be required which would amount to $165,600 (not accounting for the possibility of multiplexing); and this would still leave longitudinal cracks at risk of being missed. The focused beam of the laser helps with reflection from light colored objects such as aggregate. This could also be an ideal candidate for verification of a crack in the pavement. The ruggedness of this sensor is such that it is used in the automobile industry for vehicle suspension studies.

Line scanning lasers usually involve a laser source, a rotating mirror, and a receiver. Currently, a line scanning laser is under development to measure the reflective properties of road markers within the Caltrans/UC Davis Advance Highway Maintenance and Construction Technology (AHMCT) Program. Whether this laser would work for detecting cracks is uncertain as the intensity of

the reflectance can change due to many varying surface conditions which are not cracks; i.e., single reflectance values alone to not distinguish cracks.

Another sensor involves the use of a laser as a radar component to achieve 3-D images; this sensing method is termed Lidar. Lidar systems obtain three-dimensional information by interrogating a scene with a beam of light, typically a laser pulsed or modulated in some way. The light reflects from the subject, returns to a receiver system, and is detected. Distance information is obtained by determining the time it took light to travel to the object and back or by measuring the phase angle of the returning system. Three developers are currently known: ERIM, Odetics, and Digital Optronics. Excluding signal processing hardware, the laser units that satisfy the data acquisition rates required are in excess of $100,000, they are produced on a limited basis, and they are not rugged.

Array detectors in the visible range are used by cameras. The state of the art in cameras involves the use of CCD (Charge Coupled Device) sensors which come in line scan and area scan formats. These sensors are lightweight, require little power, and are very rugged. CCD sensors can also be sensitive to areas outside of the visible range such as the ultraviolet region and infrared region. Fairchild Weston manufactures both ultraviolet sensitive and infrared sensitive CCD array sensors. With a camera gathering images in the visible region, cracks can be identified by converting the image into gray levels (black to white level of intensity). The value of a gray level of a cracked portion of the pavement can be found by assuming that it is darker than the rest of the pavement. The crack can then be extracted based on the "darker" portions of the image. Currently data about cracks is acquired using cameras and image processing by several contractors for determining the condition of pavement. Algorithms are used to reduce noise in their image and perform histogram based analyses in order to

determine type and severity of cracking. This is a statistical process and requires no detailed correspondence between actual cracks on the road. Much development is also occurring in industrial applications of image processing. The application usually involves checking orientation of parts moving down a conveyor belt or inspection of items for defects. This is also where line scan cameras are most often used. A line scan camera most often utilizes a single line (as opposed to an array) of CCD elements in order to synchronize image acquisition with a continuous process. Carnegie Mellon's work in crack detection involves the use of machine vision with the use of a stationary array camera (Haas, C. and Hendrickson, C.T., 1990). The machine vision initially chosen for development by Carnegie Mellon involves the use of a camera (visible) and an ultrasonic range sensor to verify cracks (Hendrickson, 1989).

A pneumatic sensor is investigated due to its simplicity of construction. An annular air flow surrounds a tube from which vacuum is measured. The tip of the cone created by the annular air flow is placed in range of the pavement. when the annular air flow is disturbed by the change in height of the pavement, the pressure in the tube changes indicating a crack or rise. The phenomena itself however is highly nonlinear and unstable. Several pneumatic sensors with different annulus sizes were constructed at UC Davis and consistent results were impossible to obtain. It is immediately obvious that the sensor is not stable enough to use in crack sensing. However, some basic research and development on the geometry of the sensor may solve this problem. Commercial use of the sensors usually involves sensing the presence or absence of large objects such as rapidly moving sheet metal during hot rolling.

No information is found for the explicit detection of cracks in AC pavement using radar. However, some work is discovered for large void detection (Bomar, 1988).

An ultrasonic sensor is not recommended for sensing cracks 1/8 in (3 mm) wide at 300 Hz sample rate due to a lack of resolution and repeatability. This has been verified by attempts of Carnegie Mellon to use an ultrasonic sensor as a range sensor.[2] One possible exception is a product called a "sonic laser". This sensor is said to achieve sample rates to 800 Hz and can resolve cracks 1/8 in (3 mm) wide as long as the sensor traverses the crack normal to its direction. The difference between the sonic laser and other ultrasonic devices which are used mostly for level detection is the operating frequency. The Ultrasonic laser operates at 140 kHz whereas the standard operating frequency for most ultrasonic sensors is 30-50 kHz. The sonic laser type sensor seems as though it could be applicable as a range sensor.

No alternatives have been investigated for sensing in the ultraviolet region at this point. However, CCD cameras that are sensitive in the ultraviolet region could be employed should there develop some property in the ultraviolet range which would help to identify cracks.

Of the media mentioned, the 3-D Laser looks like the best solution as it is capable of obtaining actual road profile information. However, economy of cost and lack of robustness currently prohibits its use. Since the use of cameras associated with crack detection is an active area of commercial application, future development and system support could be expected in this area. Furthermore, if line-scan cameras are used, there would be future compatibility with other line scan technologies applied to continuous industrial operations, such as 3-D Laser profiling and far-infrared line scanning technologies, that are under development. CCD sensors contained in line scan cameras are also durable due to an absence of moving parts.

---

[2] Personal conversation with Prof. Hendrickson, Department of Civil Engineering, Carnegie Mellon University, 12/91

Given the activity in image processing in crack detection, the robust and non-contact character of line scan cameras, and the ability to substitute other line scanning technologies such as laser and infrared (i.e., heat sensing) as they develop, the use of line scan technology in the visible range is the most appropriate choice for the development of crack detection capabilities for the crack sealing machine.

1.5 Previous Work

Previous work of selected references is discussed in some detail followed by a generalization of the methods employed, and the rationale for an alternate algorithm and hardware for an Automated Crack Sealing Machine (ACSM).

The main emphasis of Bomar, et al. (1988) is to develop a working prototype video frame analyzer and identify the problems associated with enhancing and extracting surface distress features from the video data. Their video analysis software consisted of two major components: a feature enhancement process and a feature extractor. The feature enhancement process serves to increase the contrast between the desired features and the surrounding background. Enhancement is performed with the use of a convolution called the Sobel operator. The intensity levels in the image are then reversed through the use of a look-up table. An undesirable affect of the Sobel Operator is the creation of a large amount of "speckle" noise in the image. This is because there are allot of "edges" in an image such as aggregate and shadows caused by small voids. Once the edges are enhanced, a threshold is implemented to determine the cutoff point for dark pixels that are assumed to be cracks. The threshold value is selected by the operator and it is mentioned that calibration would be required.

Results showed the ability of the algorithm to detect and classify a crack is largely dependent on actual contrast conditions and resolution of the video acquisition system. However, the frame analyzer is able to identify cracks as small as 1/16 in. (1.6 mm) in 4 ft by 4 ft (1.2 m by 1.2 m) video data frames using a 512 x 512 pixel video camera taken on a continuously reinforced pavement (I-95 near Brunswick, Georgia). The surface of the roadway used is dark in color and had very thin cracks (1/32-3/16 in. (.8-4.8 mm).

The video system implemented by Bourley (1985) consisted of a CCD camera with pixels representing .33 mm x .28 mm (.013 in x .011 in) in the image are used to detect cracks approximately .1 mm (.004 in) to .2 mm (.008 in) in width. Cracks on eggs are found using four procedures in sequence: Find-Edges, Remove-Strays, Find-Contours, and measure perimeters. The image that is input is thresholded immediately by a fixed threshold. Find-Edges deletes black pixels that are completely surrounded by other black pixels. Remove-Strays deletes (maps to white) pixels that are surrounded by its four closest neighbors either completely by white pixels or completely by black pixels. Find-Contours creates linked lists of eight neighbor pixels. Lists more than 16 pixels long are accepted. The perimeters of the contours are then measured and perimeters that exceed 30 pixels are called cracks. The coordinate of the egg is interpreted as the centroid of the perimeter pixels. Mesh screening is also used here to do initial screening of crack images. This is performed by initially only looking at data in a grid pattern for locating pixels.

Results on paper strips showed as small as .5 mm (.02 in) cracks are detected (in the .33 mm (.013 in) resolution direction). With eggs and structured lighting a 25% failure rate is obtained.

Fukuhara, et al. (1990) divided a pavement image into 32x32 pixel "slits" and gray scale projections are measured with an array of processors. Excepting

this feature, the work is not documented well enough to determine the method employed. Stated results mentioned detection of cracks 1mm in width. Results are not qualified otherwise.

The algorithm employed by Maser and Schott (1981) obtained a histogram of the entire image. If the histogram is bimodal, a single threshold corresponding to the minimum between the two peaks is chosen and the image is thresholded. If the histogram is unimodal, histogram equalization is performed in order to increase the contrast of the image and spread the gray values so that the thresholding operation can be performed at one percent of the peak value. Either way, the image is thresholded based on image histogram information. With a binary (mostly white with scattered black pixels) image at hand, filtering to remove noise is performed. An 8-neighbor survivor criteria is used for binary filtering. This means that in order for an individual pixel to remain in the thresholded image, it must be completely surrounded by other (black) pixels. The remaining pixels are then dilated and eroded with a 3x3 window operator in order to link sparse features. At this stage of processing it is assumed that only significant features exist in the image, i.e. real defects. The results are based on the processing of several images. The algorithm detected all dark prominent features in image satisfactorily, i.e., cracks and potholes.

An algorithm employed for detecting cracks by Mahler (1985) used two steps. The first step is to determine if there are cracks present in an image (image selection), and the second is to specifically detect cracks in selected images (crack segmentation). Three methods are specified for image selection. All three involve the use of a reference image. This first involves the subtraction of the image histograms. The second involves the subtraction of 2-D Fourier Transforms. The third method involves the comparison of the co-occurrence matrices of the two images. For images that are significantly different (this

criteria is not specified), the differences are tested to assure that differences are occurring in the dark region. Several techniques are suggested that include the manual selection of threshold levels. Most of the suggestions are speculative, however, and provide no real information. No results are cited and the focus of the report is a design recommendation which is not based on any known performance in actual crack detection.

The crack detection method of Haas and Hendrickson (1990) is based on a thresholded image at gray scale value of 100 (256 total gray scale values). The next step is to apply a median filter. Next, the image is skeletonized (thinned out, similar to dilation and erosion). Finally, pixels that are adjacent (not including diagonal spacing) and have only one missing pixel between them are joined by filling in the missing pixel. Results obtained on a simulated laboratory crack showed promise.

The primary feature for locating cracks is crack starting location. This location is to be found within one inch (25 mm) of the edge of the crack starting location. Line scan cameras are chosen as the appropriate technology for this application. This choice is supported by the activity in image processing in crack detection, the robust and non-contact character of line scan cameras, and the ability to substitute other line scanning technologies such as laser and infrared (i.e., heat sensing) as they develop.

With respect to the algorithm to be used on the image data acquired, an algorithm will be developed that will measure the contrast in local regions and determine the continuity of high contrast local regions within the image. No preprocessing of the image is required for the method employed as has been in previous attempts at algorithm development. All of the methods employed by previous investigators using image processing (with the exception of Fukahura, 1990) use some form of thresholding as a preprocessing step in their algorithm.

The investigator feels that this step is cumbersome in that a priori knowledge of the scene is required. Even automated thresholds obtained either on a local or complete image basis still infer that all dark features in an image are cracks which inevitably leaves algorithms scrambling to clean up noise due to an assumption that is too liberal. The attendance of a lecture series at UC Davis which included Nobel Laureate Francis Crick gave some insight to human awareness that helped direct a rationale for initial algorithm development. The content of the lecture can be found in (Crick, 1990). The lecture brought out the fact that human perception is driven in part by locally dependent contrast within a scene. From my own experience, I could see that cracks are not defined by "dark pixels" but are collections of local high contrast regions directed along a relatively continuous path. A good algorithm would be one that makes use of these qualities in an integral manner.

CHAPTER 2 - MACHINE VISION DEVELOPMENT

The algorithm used to process image data is the central component of machine vision employed in detecting cracks. However, the algorithm depends on the quality of the image acquired affected by image acquisition hardware and lighting conditions. To account for these dependencies, an algorithm is developed in isolation by considering the crack as a high contrast feature within an "ideal" digital image. Following algorithm development, hardware and lighting recommendations are made intended to preserve important pavement crack features during the process in which they become part of a digital image.

2.1 Algorithm Developed for Crack Detection

The crack sensing requirements indicate that most importantly, *Location*, information is required. In order to extract this information, a histogram based approach has been developed. Fundamentally, the histogram based approach applies four operations:

1. Divides the pavement image into a *grid* of which the mesh (tile size) depends on speed requirements, desired resolution, and acceptability of falsely recognized cracks.
2. Builds a *histogram* representing each tile.
3. Computes a *statistical moment* of each histogram.
4. *Compares local values* of statistical moments to identify cracks.

The spatial relationship that is important for this method is among tiles, not individual pixels. This provides segmentation of the imag desired areas) on a macroscale, representative of human percept 1990). To follow is a more detailed description of

Grid

A video image is assumed to be created of the pavement with a pixel resolution sufficient to resolve a 1/8 inch (3 mm) feature. In order to satisfy the Nyquist sampling frequency, this requires a pixel for at maximum every 1/16 inch (1.6 mm) of highway pavement. A grid of tiles is then created to carry information about pavement features contained within a finite area. This approach has been used previously in pavement-distress-survey systems, and Ritchie, et al. (1991) have discussed the evaluation of types of cracking within tiles.

Each tile within the grid is represented by 32x32 (1024) pixels. Through the building of a histogram and the computation of the statistical moment, the data representing each tile can be reduced from 1024 counts of 8 bit data (8192 bits) to one 32 bit integer (statistical moment). The use of statistical moment data to determine crack presence is described in the comparisons section. Fig. 2.1 shows how the full lane width field of view will be divided into its component tiles.

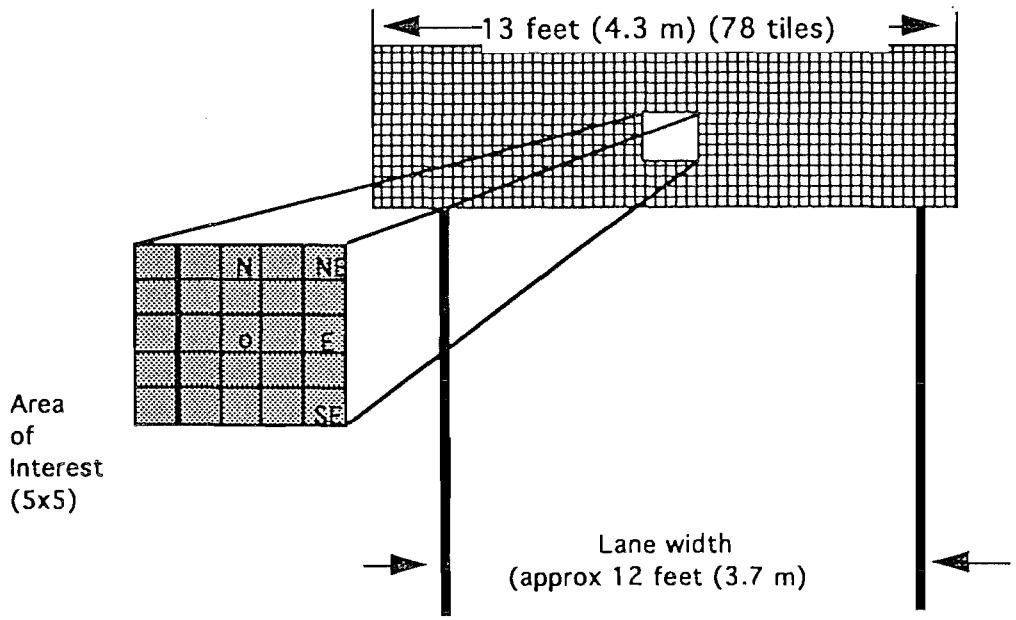

Figure 2.1
Division of Field of View into Tiles and
Four Crack Directions Within a 5x5 Area of Interest

Histogram

The first step in recognizing cracks within an area of interest is to develop a histogram for each tile. A histogram presents information on the number of pixels (digital picture elements) at particular gray levels within an image. Gray level values are a measure of the intensity of a pixel and range from black (gray level 0) to white (gray level 255 for an 8 bit image). In particular, the histogram that we use is a distribution of gray level values within a particular tile. Tiles which have cracks in them will have a greater number of darker gray level values than neighboring tiles. Fig. 2.2 illustrates histograms of two specific tiles, one with a crack and one without a crack. Histograms are widely used in image processing and they have been previously employed in pavement-distress-survey systems (see Bomar, 1988 and Mahler, 1990).

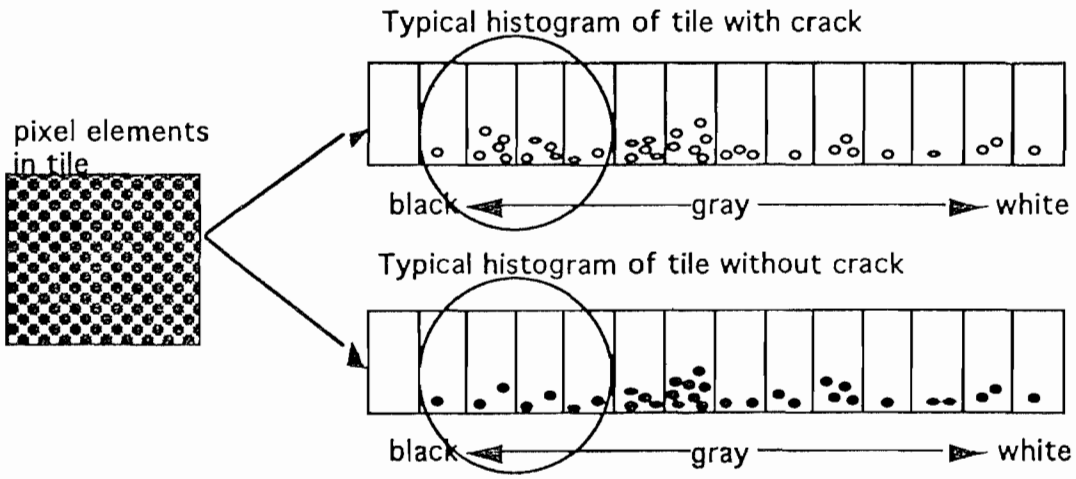

Figure 2.2
Typical Histograms of Cracked and Non-cracked Tiles

Statistical Moment

As shown in Fig. 2.2, there is a distinct difference between the histograms of tiles with and without cracks. The next task is to then represent these differences in a manner that can be easily interpreted automatically by a computer. Statistical moments have been widely used to provide abbreviated

quantitative information on large sets of data, and there have been many engineering applications using this approach; e.g., see Vinh, et al. (1985) who use statistical moments to identify nonlinearities in structures.

In the proposed approach, the mode of the histogram data is used, which is the most frequently occurring gray level value corresponding to the peak of the histogram. Then only pixels darker than each tile's are used to compute the statistical moment of this data relative to the mode for each tile. In general there are an infinite number of statistical moments. In this case, m_e, the e'th statistical moment of the data, is represented as

$$m_e = \sum_{i=0}^{Mode} r_i^{\,e} n_i \qquad (2.1)$$

where i denotes the gray scale value, n_i denotes the number of pixels in the tile at that gray scale value, r_i represents the gray level distance from the mode to the i'th gray level, e is the power to which the r_i are raised, and note that the sum includes only those gray level values less than the mode. These parameters are depicted in Fig. 2.3.

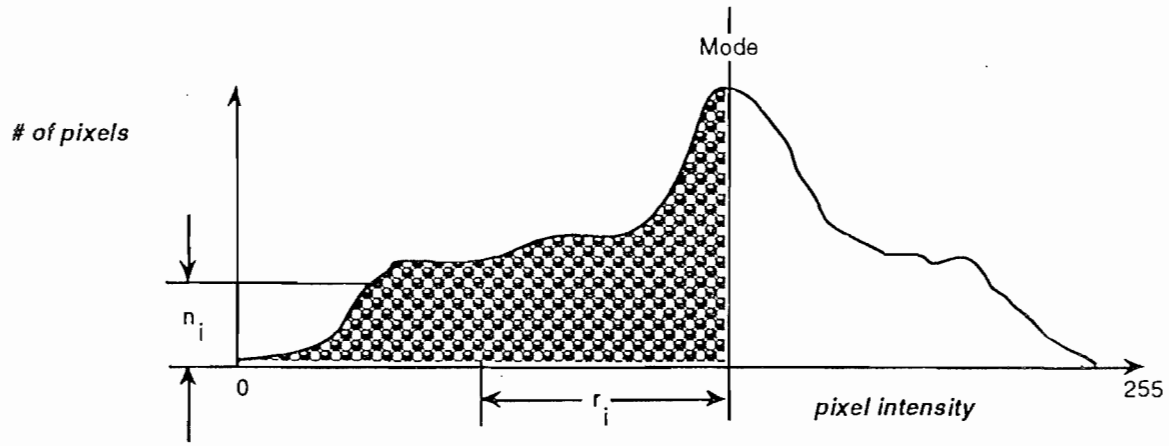

Figure 2.3
Histogram Depicting the Parameters Employed in the Statistical Moment Computation

By taking statistical moments relative to the mode, a measure of deviation from the most common intensity is effectively developed. For this application, the mode represents the background (pavement) against which the cracks will be recognized. For uniform sections of pavement (i.e., those without cracks), one would expect a relatively narrow distribution of intensities regardless of the lighting. As such, the statistical moments of tiles with a crack will deviate from those for tiles without cracks with relatively minor sensitivity to type of pavement and lighting. That is, this approach has the potential to be extremely robust in comparison to the numerous methods that threshold data; i.e., select a particular pixel value above which data records are disposed of. Preliminary investigation has shown that the third statistical moment (corresponding to value of e=3) allows significant distinction between cracked and uncracked tiles for a variety of pavement types.

The tile size of 32x32 pixels allows for a minimal amount of variation in local* modes by reducing the effects of intensity changes within tiles due to differing shades of aggregate and surface defects. A small variation in local modes allows for a comparable measure of darker gray level values among adjacent tiles. This characteristic of local modes is what specifically allows for the recognition of cracks based on statistical moments about modes. If local modes varied substantially, local statistical moments would not be comparable. Reducing the variation of local modes with larger tile sizes must be weighed against the required accuracy to perform a sealing operation. Too large of a tile size may not provide the resolution required for a given operation.

---

* Local is defined as a 5x5 grouping of tiles. This is the minimum number of tiles required to identify the eight directions that we have elected to recognize. These directions are elaborated upon in the comparisons section.

Comparisons

Once computed for each tile, the statistical moment values are compared within independent 5x5 tile areas. The principle function of our method is to recognize a grouping of tiles which have a greater amount of contrast, which is represented by the statistical moment value, relative to neighboring tiles. Specifically, the steps are as follows:

- A set of 5x5 tile areas of interest is considered such that every tile in the grid (with the exception of the two columns of tiles on either end) is considered once as the center tile. Fig. 2.1 denotes the center tile location as **o** and shows four of the possible eight directions for an individual 5x5 area of interest.
- For each individual 5x5 tile area, a set of conditions are invoked in order to determine both the presence of a crack and its preferred direction. The conditions are best illustrated by referring to Fig. 2.4. In order for a crack to exist, all of the statistical moment values of the **D**irection tiles (labeled as **D**) as well as the moment value of center tile (**o**) must be greater than all of the statistical moment values of the **C**omparison tiles (labeled **C**) for that individual crack direction. The **D** tiles have been chosen to resolve the crack into eight possible directions. The **C** tiles have been selected based on experimentation such that the possibility of a **C** tile sharing a crack with a **D** tile is minimized.
- The conditions for the eight directions are tested sequentially from North (N) to South East_North (SE_N), with the first recognized direction remaining as the recognized direction if more than one directional condition is met.
- If any condition is false, i.e., any **C** > (**D** or **o**) for a direction, it is determined that no crack exists along that direction.

Note that there is significant overlap from one 5x5 area to the next; i.e., since each tile is a center of a 5x5 area, there will be an overlap of four of the five columns between adjacent areas of interest. Thus, there is redundancy in capturing a crack along its length. Fig. 2.4 shows the comparison criteria within

5x5 areas for all eight directions. Although direction and length information could be provided by the machine vision system. Crack locations implied by extremes of groupings of tiles recognized as cracks would probably be sufficient allowing details of crack length (and intersections) to be determined by a path planning function outside of the machine vision system. This creates a hierarchy of functions, specializing the machine vision in finding crack locations only.

Regarding real-time operation required for the ACSM, the tile size employed in this approach is consistent with the scale of the defects to be recognized. While microscale (pixel) information is employed in establishing the characteristic of a tile (statistical moment), it is not necessary to retain all the microscale information and thus, real-time operation is feasible.

2.2 Hardware Selection

The operation of the machine vision system is required to run at 2 miles per hour (3.2 km/hr) in a continuous fashion. This means that the pixel data must flow continually through the system without interruption. A system that meets the requirements is described below. The principles of operation of this system are sequentially described in Fig. 2.5, and detailed operation follows.

The wheel encoder is an opto-electronic device that translates vehicle wheel rotation into electrical pulses. This is accomplished with the use of a light emitting diode, a template, a photo diode, and squaring circuitry to threshold a sinusoidal response of the photo diode. The operation of the wheel encoder is graphically described in Fig. 2.6.

The pulses that are created by the encoder would be used to synchronize the acquisition of road image information. This is to assure that for differing vehicle speeds, the image information will represent a properly scaled image of the road. The image processing hardware must be capable of detecting the

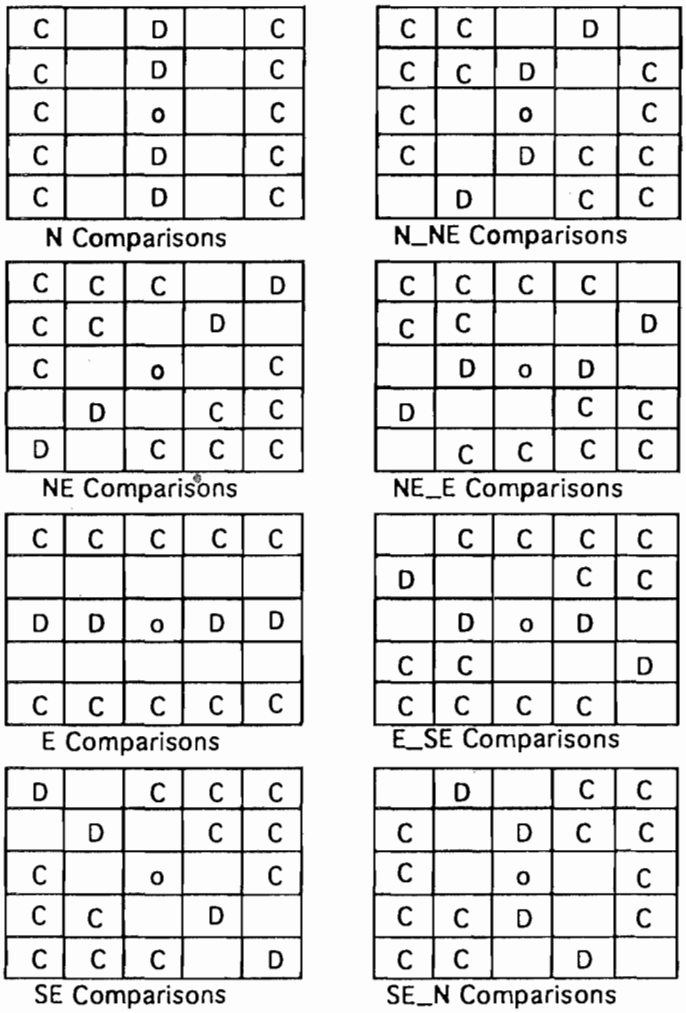

Figure 2.4
Summary of Comparisons for Crack Direction Determination

beginning or ending of each individual pulse so that a line of video can be acquired for each pulse. On a typical truck tire the rolling radius is approximately 15 in (38 cm) which will provide a pulse every 3/32 in (2.4 mm) with a 1000 pulse per revolution encoder which falls short of the Nyquist sampling criteria by 1/32 in (.8 mm). This however should be sufficient for initial testing purposes.

In order for the image processing hardware to synchronize wheel rotation and camera acquisition, it must have two important functions:

1. Horizontal edge detection circuit, and

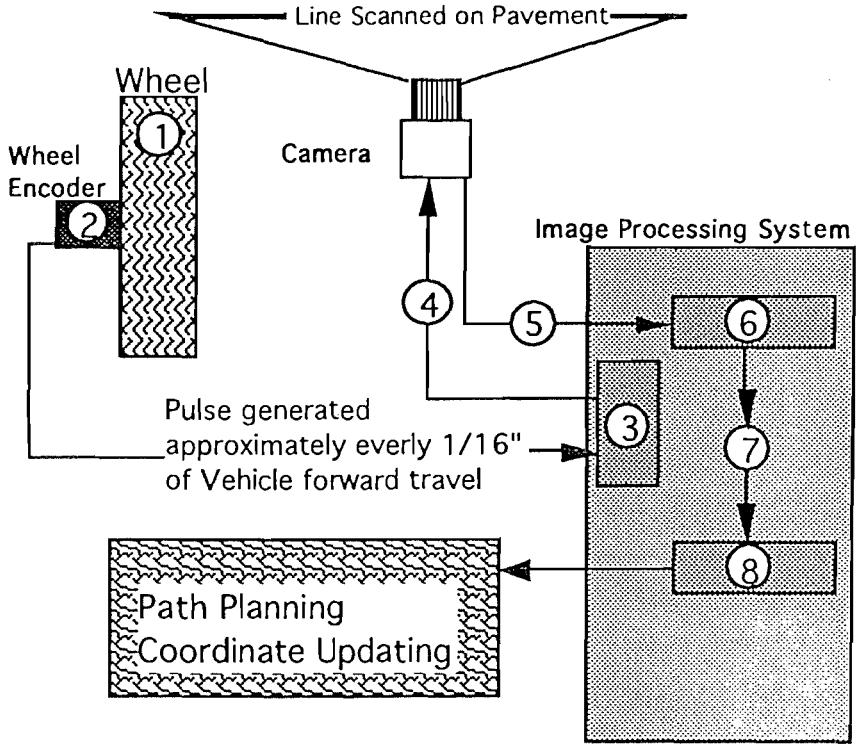

(1) Wheel rotates an incremental amount
(2) Encoder produces a pulse resulting from incremental vehicle travel
(3) Image processing hardware reads pulse from encoder and
(4) Sends control signals for camera to acquire video line and
(5) return a video signal representing one line of pavement back to the
(6) Image Processing Hardware
(.....*this procedure iterates until enough lines are gathered to determine crack presence at which time* .....)
(7) An Algorithm* determines crack presence in image and transmits crack information to
(8) A communications device which communicates the crack information to a path planning function (external to the global machine vision).

*-For algorithm specifics, see Algorithm Details

Figure 2.5
Hardware Principles of Operation

2. A "look up table" counter to synchronize camera and image processing hardware

These two functions are shown as block three in Fig. 2.5. This "front end" block of the image processing hardware receives pulses from the encoder and executes a predetermined set of instructions in the form of a look up table. The functional description of the image processing front end is shown in Fig 2.7.

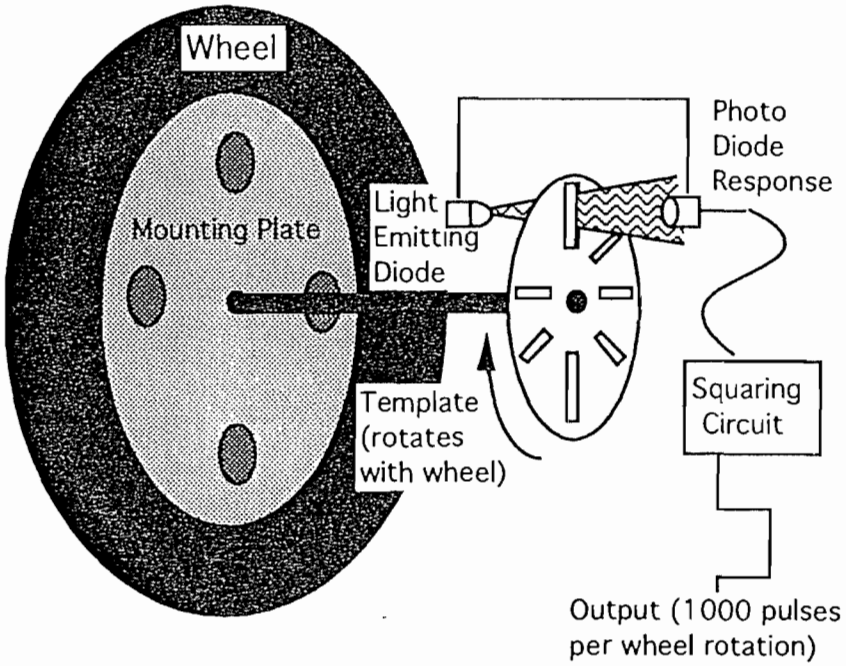

Figure 2.6
Functional Breakdown of Optical Wheel Encoder

As can be seen from Fig. 2.7, the encoder pulse resets a counter. For each proceeding count value (driven by the clock input) there is a preprogrammed state for the control lines that perform functions such as the integration of the camera, position determination in the image processing pixel memory, etc. The actual states of a look up table (HLUT or horizontal look up table) depend on vendor specific hardware. For the implementation of this machine vision concept, a Fairchild line scan camera and a Data Cube image processing front end are recommended.

The count of the counter is called the "operand" and the values of the control lines are called the "states". For camera integration, bit 3 of the counter can be used. When the camera is integrating, the vehicle is moving forward and some smearing occurs. This smearing should be limited to 1/16 in (1.6 mm) so that significant averaging (which would tend to smooth out dark spots) would not occur.

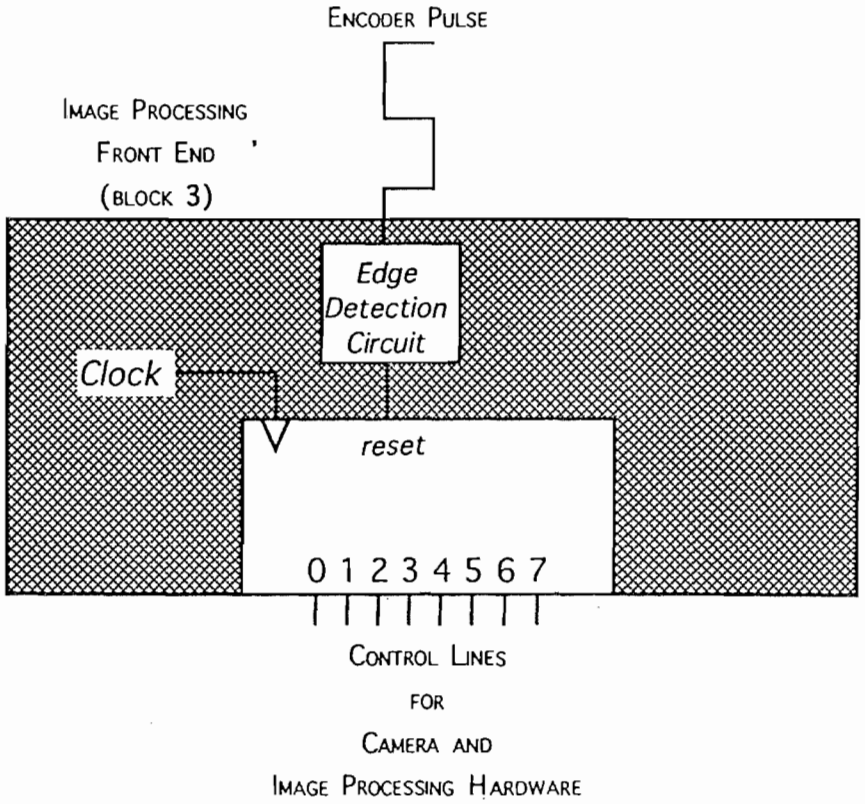

Figure 2.7
Image Processing Front End

Due to the limitations of camera resolution and the field of view of the road to be imaged, two cameras are required. Fig. 2.8 gives a pictorial description of the averaging and offset of video information that occurs with two cameras.

During integration the charge coupled device (CCD) sensor on the camera accumulates charge from incident photons. Fig. 2.9 shows the principle of operation for a CCD sensor in general. The front end of the vision system uses the reference cells to determine the zero voltage reference for the video signal. This is called the "DC restore" in the digitizing process.

The above mentioned hardware has been purchased by Caltrans in the development of an Automated Crack Sealing Machine (ACSM). Conceptually, the hardware seems to support a continuous operation.

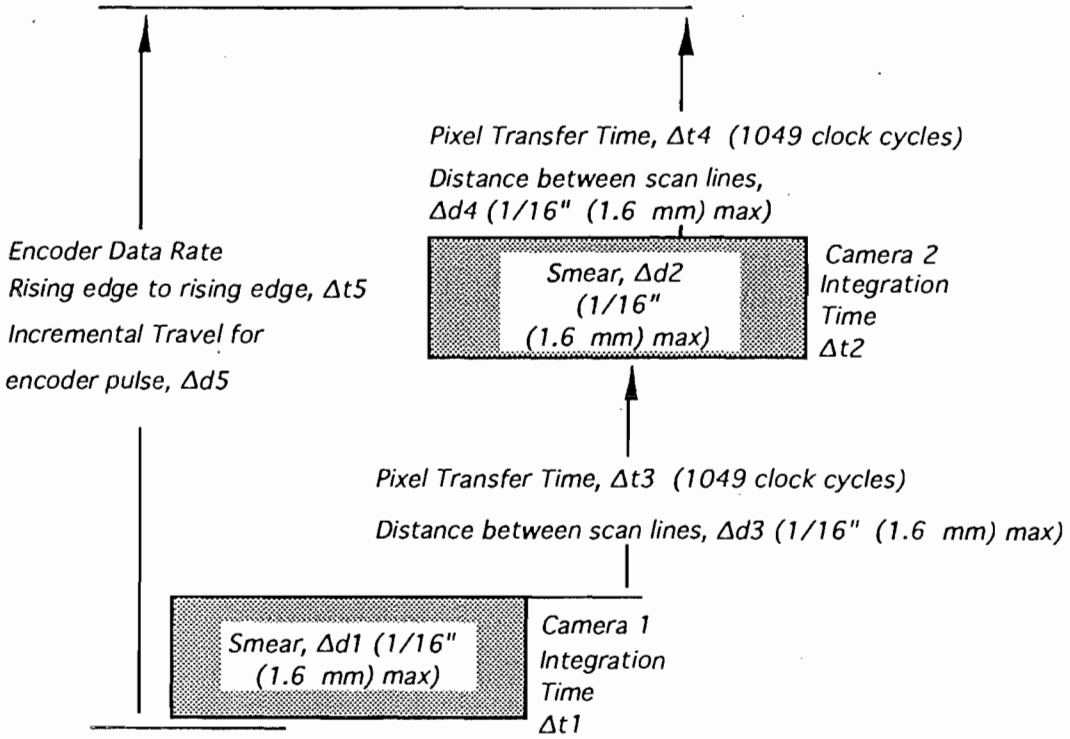

Figure 2.8
Graphic of Image Smear During Integration

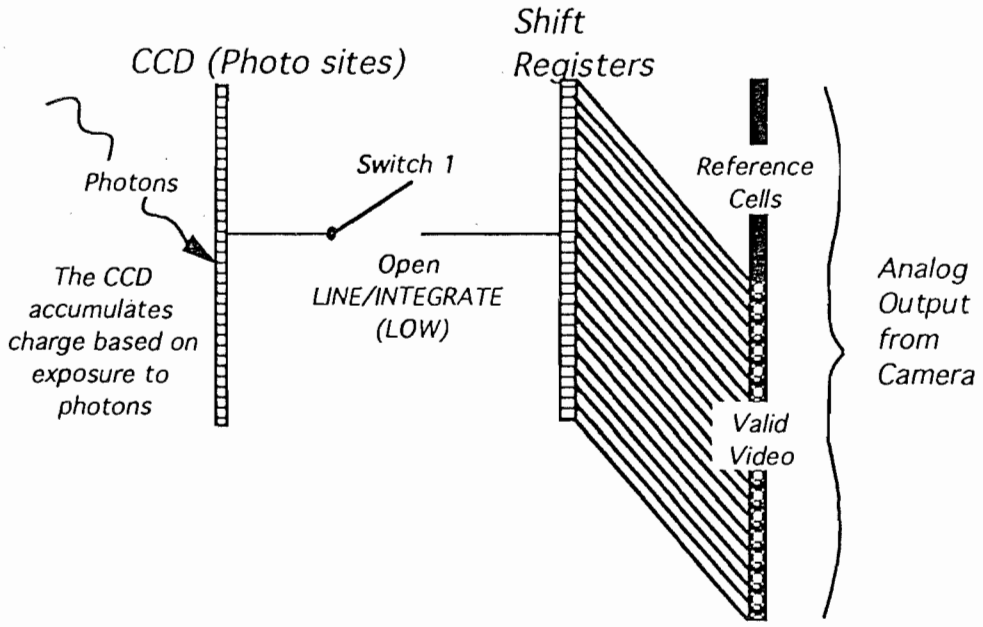

Figure 2.9
CCD Principle of Operation

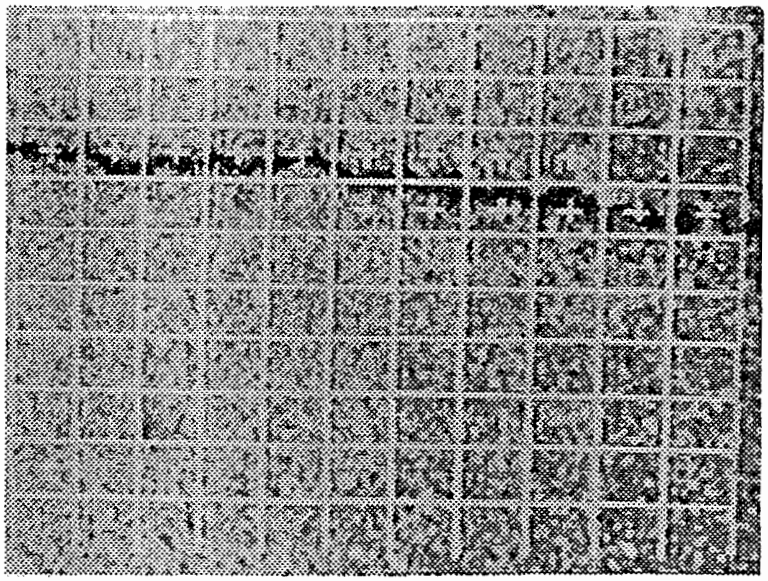

Figure 2.10
Preliminary Algorithm Results for a Transverse Crack

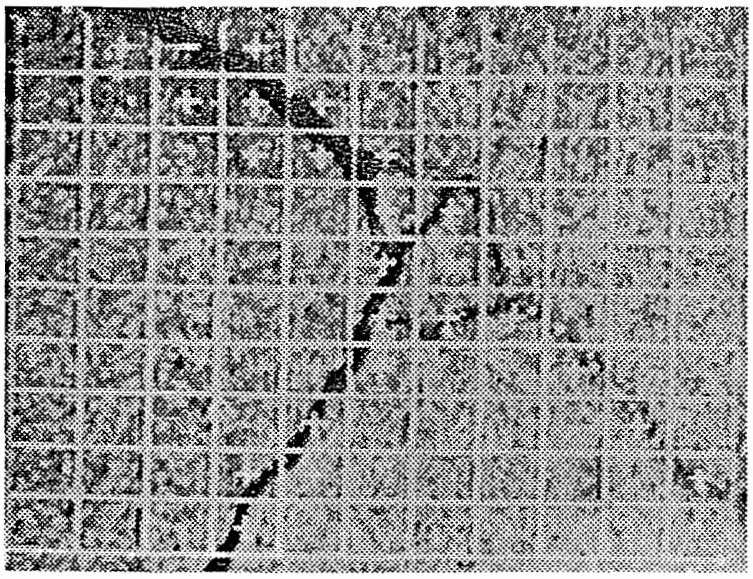

Figure 2.11
Preliminary Algorithm Results for a Crack with
Varying Widths and Debris

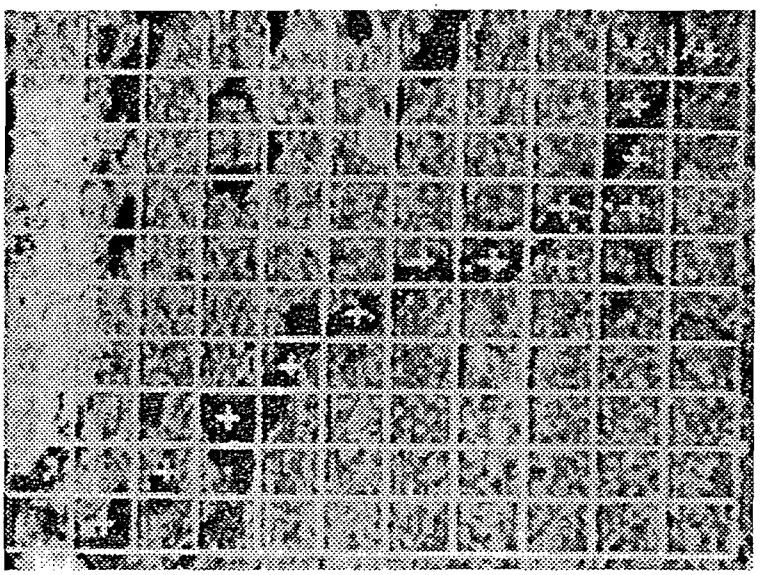

Figure 2.12
Preliminary Algorithm Results for a Crack with Oil Spots

2.3 Lighting Considerations

Extensive work on the lighting of pavement for the purposes of crack detection has been performed by El-Korchi and Wittels (1990, 1991). Specific recommendations are to create an illumination environment where the lighting quality is as diffuse (i.e., omnidirectional) as possible. Another consideration is the amount of illumination. The amount of illumination is dependent on the cameras and optics employed. However, assuming that there is enough light for the CCD(s), the quality of the lighting determines the suitability for crack detection purposes. The following criteria are relevant in the development of the lighting on the ACSM :

- The goal of the lighting will be to provide significant illumination for two Fairchild line scan cameras whose focal planes will be mounted approximately 6 feet (1.8 m) perpendicular to AC (dark asphaltic) pavement each with a field of view of 6.5 feet (2 m) in such a manner that the cracks will be accentuated. The illuminated area will be a

maximum of 13 feet (4 m) in width with a maximum width for traveling to and from a job site of 8 feet (2.4 m).

- The cameras used will be Fairchild CAM 1301R line scan cameras with JML P/N 71846 (12.5mm, f1.3) lenses. The integration time for the sensors will be approximately .7 milliseconds at a line rate of approximately 576 Hz

- The lighting should provide for approximately 50-75% of sensor saturation over AC pavement.

In order to get a feel for the lighting requirements a bench test is performed to determine lighting requirements for a scaled down test. Based on this test, it approximately 14, 1000 Watt light sources would be required to illuminate the pavement for the ACSM. This lighting requirement is severe due to the poor reflective properties of AC pavement and a long distance (6 ft (1.8 m)) that the cameras must be placed above the pavement. Lighting requirements could be reduced significantly by fiber optically coupling the cameras allowing several lenses (therefore, several smaller fields of view) to be placed much closer to the pavement.

A detailed algorithm concept has been developed for crack detection. Although the algorithm is intuitively appealing, testing must determine its promise for use in the ACSM to find crack locations. Hardware has been recommended for the acquisition and processing required for a continuous operation. A preliminary determination has been made regarding lighting requirements.

Although full-scale hardware integration and lighting are required to test the machine vision for use on the ACSM, the algorithm as the kernel of the machine vision system can be tested with standard image processing hardware in a stationary laboratory environment.

CHAPTER 3 - MACHINE VISION TESTING

The focus of the machine vision testing is to exercise the algorithm and lighting concepts within image processing hardware limitations. Furthermore, variations of the algorithm and algorithm parameters are tested in a structured experiment in order to determine sensitivities relating to performance.

The image processing hardware and lighting considerations are addressed first conceptually as system performance factors. System performance factors in creating a digital image are hardware resolution, crack geometry, lighting quality, and their combined effects. The measurement of these performance factors will quantify: spatial resolution (in inches (mm)), gray scale resolution (as a gray level value tolerance), and lighting quality (as a potential difference in gray scale values for measured crack features directly from the sample). Once measurements are made software performance is measured with the use of variance analysis (ANOVA) techniques.

Testing is accomplished with a PC machine vision system in a stationary, laboratory environment using a cracked PCC sample. The lighting is implemented with the use of 90, 1 Watt lights that surround the sample approximately 12 inches above the sample. Fig. 3.1 shows the Panasonic industrial CCD camera, the lights circumferential to the focal plane of the camera, foil shroud to help with light intensity, and the test specimen. Fig. 3.2 shows the view of the specimen from behind the camera. The image from the camera is acquired by a Matrox MVP frame grabber and the image data is manipulated with the use of an IBM-clone 286 PC. The C implementation of the algorithm is contained in Appendix B for reference.

3.1 System Performance Factors

Several aspects of the machine vision system are accounted for during testing, including: hardware resolution, gray scale resolution, lighting quality, and crack geometry.

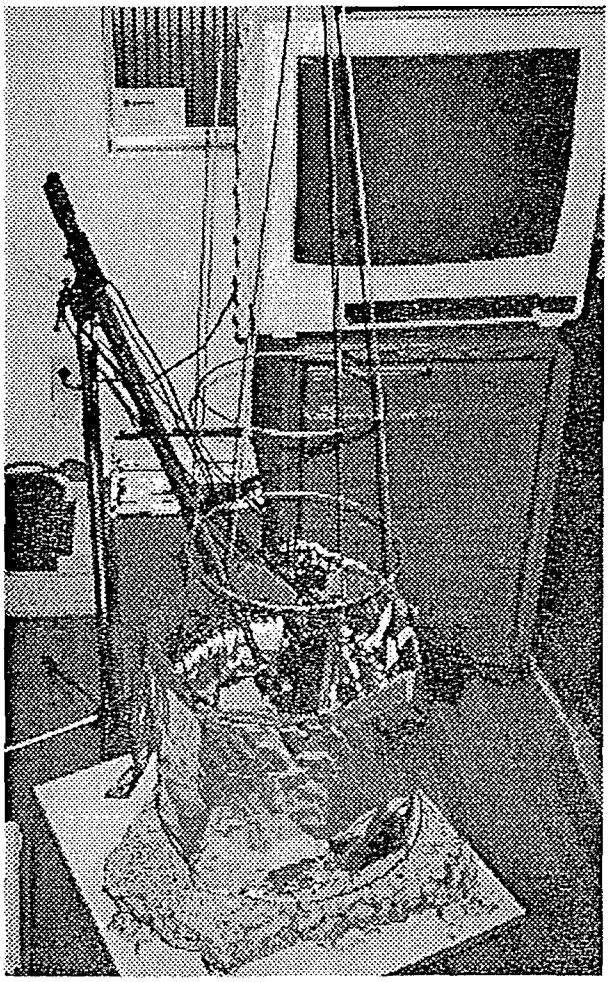

Figure 3.1
Machine Vision Test Setup

3.1.1 Hardware Resolution

The implemented algorithm depends on the performance of both machine vision hardware and software. Hardware features directly effect algorithm performance through image resolution. Image resolution is affected by spatial

sampling, gray scale sampling, and lighting quality. The software will segment image features based on the resolution provided by the imaging hardware.

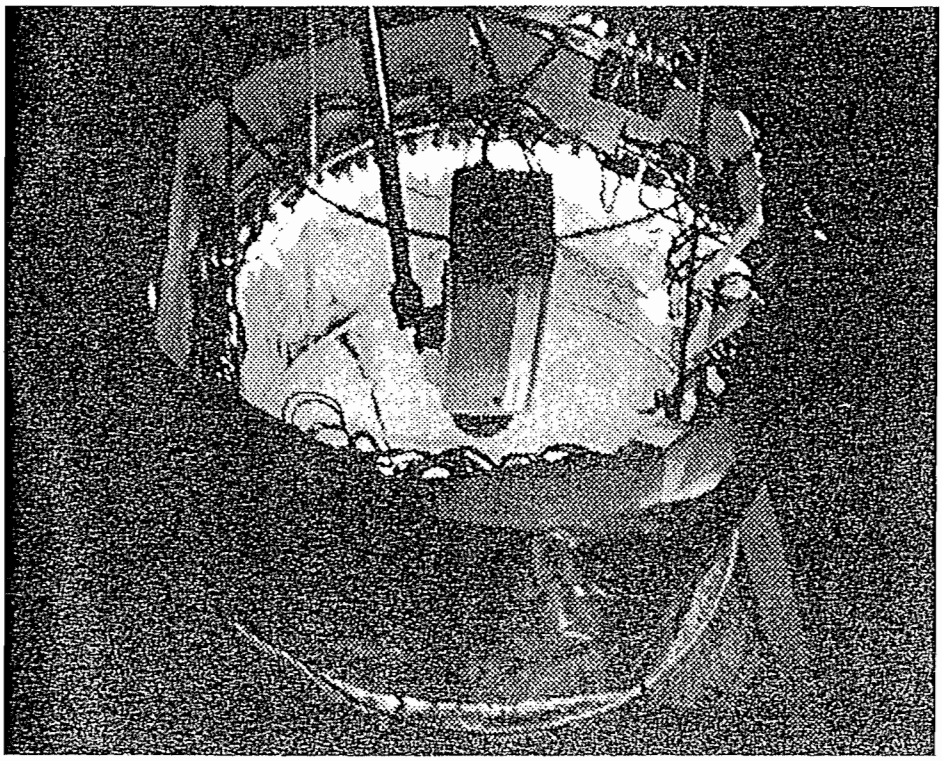

Figure 3.2
View of Specimen from Behind Camera

The imaging hardware is a measuring tool that is used to quantify the pavement image. A digital image is created by converting reflected light intensities from the surface of the pavement into 1 of 256 shades of gray. This is accomplished with use of a Panasonic model WV-BD404 standard format video camera and a PC-based frame grabber. The camera contains a CCD consisting of many individual light sensors that produce small voltages in response to photons. The voltages from each light sensor is amplified within the camera and converted at the frame grabber by an analog to digital converter to 1 of 256 shades of gray which is accessible to a personal computer. The "gray level"

values are then accessed and manipulated in order to implement the crack detection algorithm.

The challenge of the crack detection algorithm is to find a way to extract the crack feature. However, the crack detection algorithm is limited by the hardware's ability to preserve features in the scene. Features are defined by intensity and spatial qualities. The hardware communicates these interdependent qualities within the limitations of its gray scale and spatial resolutions, and its lighting environment. These resolutions can be roughly quantified by measuring a few critical items in the imaging system; spatial resolution, gray scale resolution, and lighting quality.

3.1.1.1 Spatial Resolution

The Nyquist sampling criteria is used as a spatial sampling criteria for preserving image features. This criteria requires that the sampling frequency be at minimum twice the spatial frequency of the features that are to be detected. A graphical illustration is provided in Fig. 3.3. An intensity profile to be imaged *x* in width and *y* in intensity is shown. Notice that sampling provided by an imaging system based on an x ruler (i.e., pixel size) cannot preserve the magnitude of the intensity variation across x in a typical situation where sampling occurs on the edge of the feature. This is due to pixels falling on the edge of the feature, blurring edge features in the scene.

In order for magnitude of the intensity variation along the profile to be preserved, the maximum measurement interval (i.e., pixel size) must be no greater than x/2 as shown in the *x*/2-based reconstruction in Fig. 3.3. Note that sampling at x/2 does not reconstruct a feature width (i.e., some blurring still occurs) but only preserves a maximum intensity variation across a feature width, *x*.

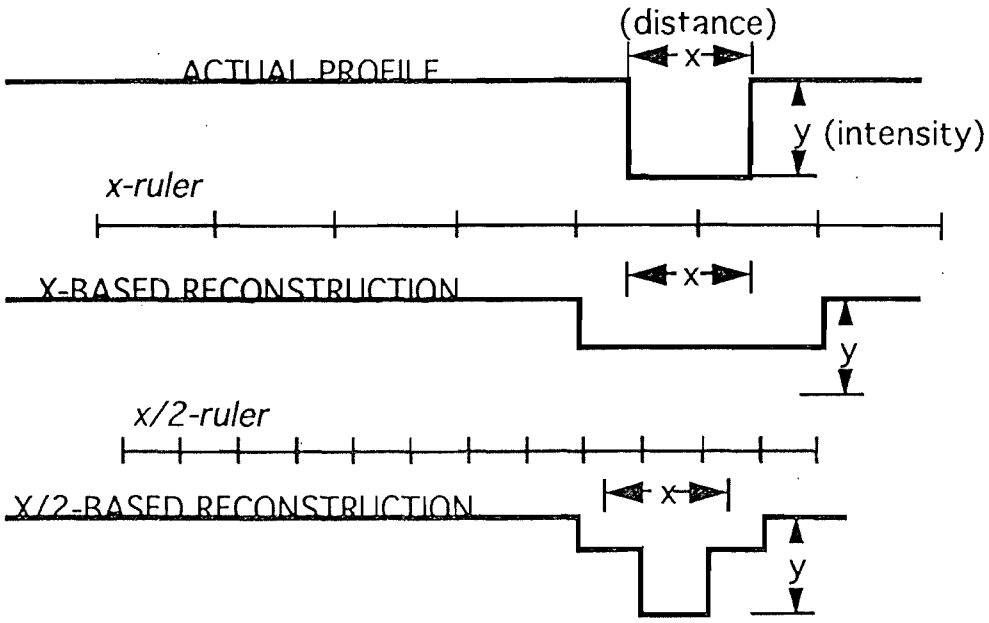

Figure 3.3
Nyquist Criteria Example

Assuming that the Nyquist sampling criteria is satisfied, the intensity variations that are present must lie within the gray scale resolution of the imaging system.

3.1.1.2 Gray Scale Resolution

The gray scale resolution of the imaging system is determined by the dynamic range of the camera and the number of gray levels created by the digitizer. The dynamic range of the camera is determined from two properties of the video signal provided by the camera which are highly dependent on the camera's CCD sensor (Charge Coupled Device). The first property of the video signal is called the noise floor (also called *random noise* or *dark current)* and the second is the saturation level. The noise floor is the electrical signal that the camera generates without any light present. The second is the saturation level which is the maximum light intensity to which the CCD sensor within the camera can respond. The left graphic in Fig. 3.4 shows the video level associated with

the random noise (N) of the camera. The right graphic shows the camera responding to intensity (N+I) at saturation which is represented by 1 volt output for an RS-170 standard employed by most black and white video cameras. Note that the dark current is part of any value measured. The ratio of the maximum intensity response of a camera to the random noise level for a high performance camera is about 300:1 which is about 50 decibels (dB) = 20*log(300/1).

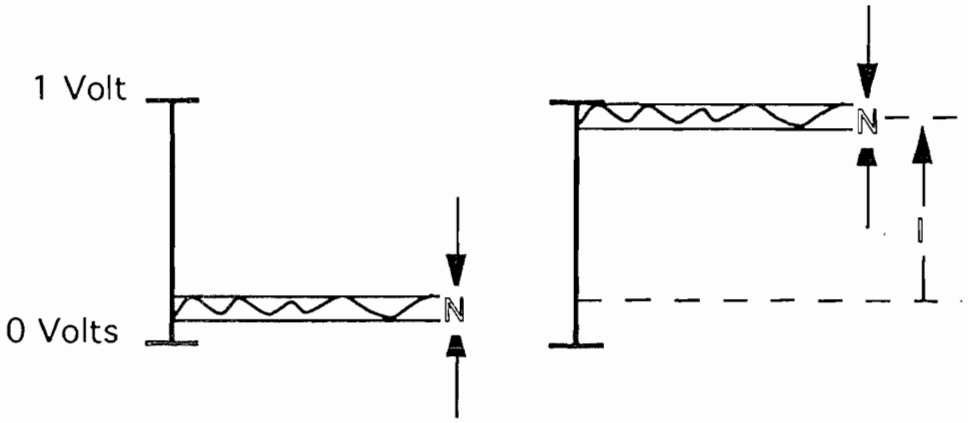

Figure 3.4
Video Level Associated with the Random Noise (N)
and Saturation (N+I) of a Camera.

The digitizer in an imaging system uses the video signal from the camera and transforms it to a gray level value. The digitizer used in the PC based system used for testing produces 8 binary digits of resolution or 256 gray level values. As illustrated in Fig. 3.5, the digitizer samples the incoming video and assigns a gray level value for each sample.

This sample will vary over repeated times however by an amount N. For a 50 dB camera (300:1) and an 8-bit digitizer (256:1), the noise from the camera is comprising 85 percent of a pixel's gray level value. The smaller this percentage

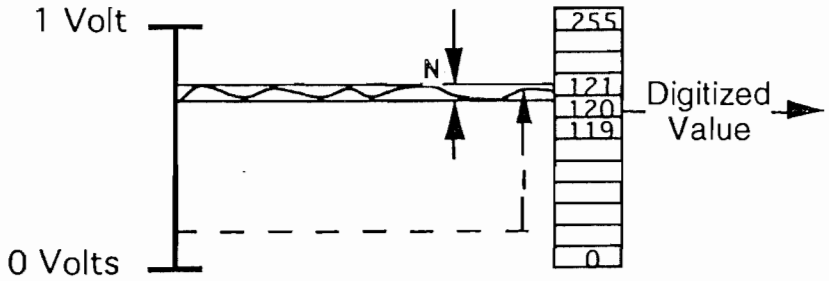

Figure 3.5
Uncertainty in Sampling

becomes, the less likely noise will cross over to an adjacent gray level value. The most conservative assumption, however is that a digitized value of 120 as shown in Fig. 3.5 could result from a video signal that was predominantly at an adjacent gray level value (121 in this case). In other words, if the digitizer has assigned a gray level value of 120, then one can only assume that the actual intensity value in the scene is somewhere between 119 and 121 or 120 +/- 1. This uncertainty in sampling means that each measurement represents a range of 3 pixels over a scale of 256 gray scale values. The resulting 82:1 (from 356:3) or 38 dB dynamic range resulting from the digitizer represents the overall gray scale resolution of the imaging system.

The implications of the 82:1 signal to noise ratio are shown in Fig. 3.6. The change in intensity, y, across the profile, x, is some pure number before it is digitized (8 gray scale values in our example). Due to the effects of spatial sampling alone, the *change in intensity* is preserved. $y_1 + y_2$ are the new intensity variations equal to 4 gray scale values. y_1 and y_2 will be further modified by digitizing due to the gray scale resolution of the imaging system. The effect, in the worst case, would be to degrade the intensity variation slightly which reduces contrast.

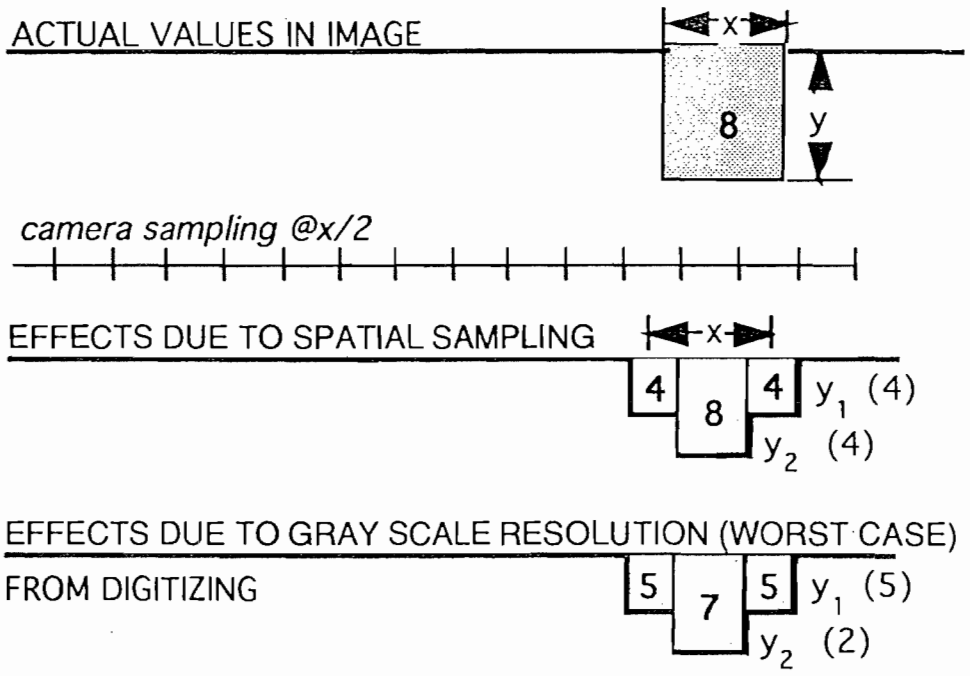

Figure 3.6
Illustration of Profile Degradation due to Spatial Sampling and Gray Scale Resolution

Assuming, however, that there is sufficient contrast due to crack geometry and lighting quality, the effect of spatial sampling and gray scale resolution should not significantly effect the contrast in the image.

3.1.2 Crack Geometry and Lighting Quality

Crack depth profile and lighting quality will determine the intensity change across a given crack segment. The operating conditions of the crack sealing machine are such that it is desired that the crack width "x" be 1/8 in (3 mm). Assuming that cracks are **"V"** shaped, the lighting quality can be considered analytically by comparing light intensity on the surface directly adjacent to the crack to the light intensity at the bottom of the crack. Fig. 3.7 shows a crack of width, W and depth, D. The half moon symbol represents the intensity at the

bottom of the crack, the full moon symbol represents the intensity on the surface of the pavement.

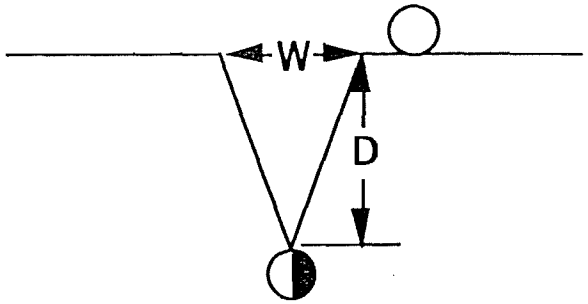

Figure 3.7
Crack Dimensions and Intensity Symbols

The difference in intensity between the full moon location and the half moon location will determine the contrast for a given crack segment. Fig. 3.8 shows in a plane that portion of omnidirectional lighting that is available to the full moon location (π) and the crack location (ϕ). This determines the contrast in the scene that represents the crack.

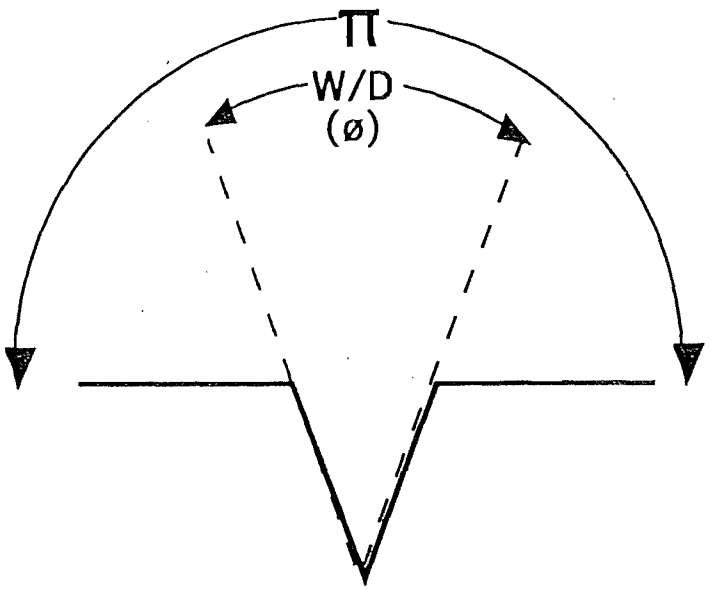

Figure 3.8
Omnidirectional Lighting that is Available to the
Full Moon Location (π) and the Crack Location (ϕ)
for Small Values of W Relative to D

This also provides the basis for the lighting contrast recommended by El-Korchi and Wittels (1990, 1991) and is equal to $(\pi-\phi)/\pi$. The lighting quality desired to achieve this value is omnidirectional light that resembles the quality of skylight (similar to a cloudy day, dawn, or twilight). This lighting quality will ensure that no crack directions receive more contrast than other crack directions as well.

3.1.3 Combined Effects

A crack that is exactly 1/8 in (3 mm) and 3/4 in (19 mm) deep will have a W/D ratio or ø equal to .16. Assuming that the modal gray level value of the pavement sampled at the surface is150 and the lighting is omnidirectional, the crack will be at a gray level value of $150*(\pi-\phi)/\pi = 142$. This theoretical value provides a difference of 8 gray scale values and by coincidence is the same value as shown in Fig. 3.6. This difference should be sufficient for crack detection as is it not likely that through hardware limitations that intensity variations would be lost.

3.2 Measurement Methods

Spatial and gray scale resolution are measured for the image processing hardware. The quality of the image obtained will define the features that are available to the algorithm for crack detection. In particular, crack width and intensity changes across the crack must be preserved for crack recognition to occur. A contributing factor towards preserving image features is lighting quality which can also be measured.

3.2.1 Spatial and Gray Scale Resolution

The effect of spatial and gray scale resolution is tested with the use of electrical tape cut in strips and placed against a dark background. The strips

consist of 1/32 in (.8 mm), 1/16 in (1.6 mm), 1/8 in (3 mm), and 7/8 in (22 mm) (reference strip) widths. The minimum value of the 7/8 in (22 mm) reference strip is determined by reading pixels values along the reference strip. The smallest strip that can represent the minimum value of the reference strip within one pixel value along the width is the hardware resolution due to spatial and gray scale resolutions. With respect to ACSM operation, the forward resolution of the image will be controlled by an optical encoder. The field of view transverse to the vehicle is covered by two cameras (Fairchild CAM 1301R line scan cameras with JML P/N 71846 12.5mm, f1.3 lenses mounted 6 feet 1.8 m from the ground). Each camera will have a field of view of 6.4 feet (2 m) and will be mounted 6.4 feet (2 m) apart. The spatial resolution across the field of view is greatest directly below each camera and it is expected that the resolution will fall off to below 1/8 in (3 mm) resolution towards the edges of the fields of view due to non-linearities of camera optics.

3.2.2 Lighting Quality

The lighting quality will be measured with the use of a Litemate II Photometer (Model 504) and a protractor. The lighting quality will be generally observed to see if it meets an omnidirectional criteria.

In summary, sufficient hardware resolution will be defined by that portion of its field of view that provides spatial resolution and sufficient contrast due to lighting in order to preserve crack features. Measured values of hardware resolution, crack geometry, and lighting quality will be used to assure this condition prior to the evaluation of software performance.

3.3 Measurements

Spatial resolution, lighting quality, and image contrast are measured in order to determine if the crack features in the image are of sufficient quality for

measurement of software performance. Image contrast is measured by recording digitized intensity profiles perpendicular to cracks in the image. The deeper and wider the intensity profiles across the crack, the higher the contrast.

Software performance is measured by quantifying the success rate in locating cracks on a tile-by-tile basis. Algorithm parameters hypothesized to affect performance are varied including moment equations, individual moment values, and an "offset" parameter found to enhance performance during initial algorithm testing.

3.3.1 Spatial Resolution

For convenience, the camera is not mounted entirely planar to the surface. As a first step a ruler is applied to the image and the relative sizes of the grids are measured in the image. Each tile represents 32x32 pixels in the image so pixel resolution could be estimated as a first step. Fig. 3.9 shows the tiles overlaid on the sample and sample tile dimensions in inches. Next to the dimensions are the approximate number of pixels per 1/8 inch (3 mm) of length.

Note that on the image there is at least 4 pixels for 1/8 inch (3 mm) of sample. This would indicate using Spatial sampling criteria alone that we have 1/6 inch (1.6 mm) image resolution.

The spatial resolution within the field of view of the camera is further examined with the use of electrical tape cut in strips and placed against a dark background of a green file divider. The widest strip is used to obtain a minimum pixel value for the tape. Using previously developed criteria in section 3.1.1 and Fig. 3.6, the resolution of the imaging system is then the smallest strip of electrical tape in which the minimum is represented within a pixel value. Fig. 3.10 shows the location of the resolution test strips. Tables 3.1 and 3.2 show two pixel readings across each segment of electrical tape.

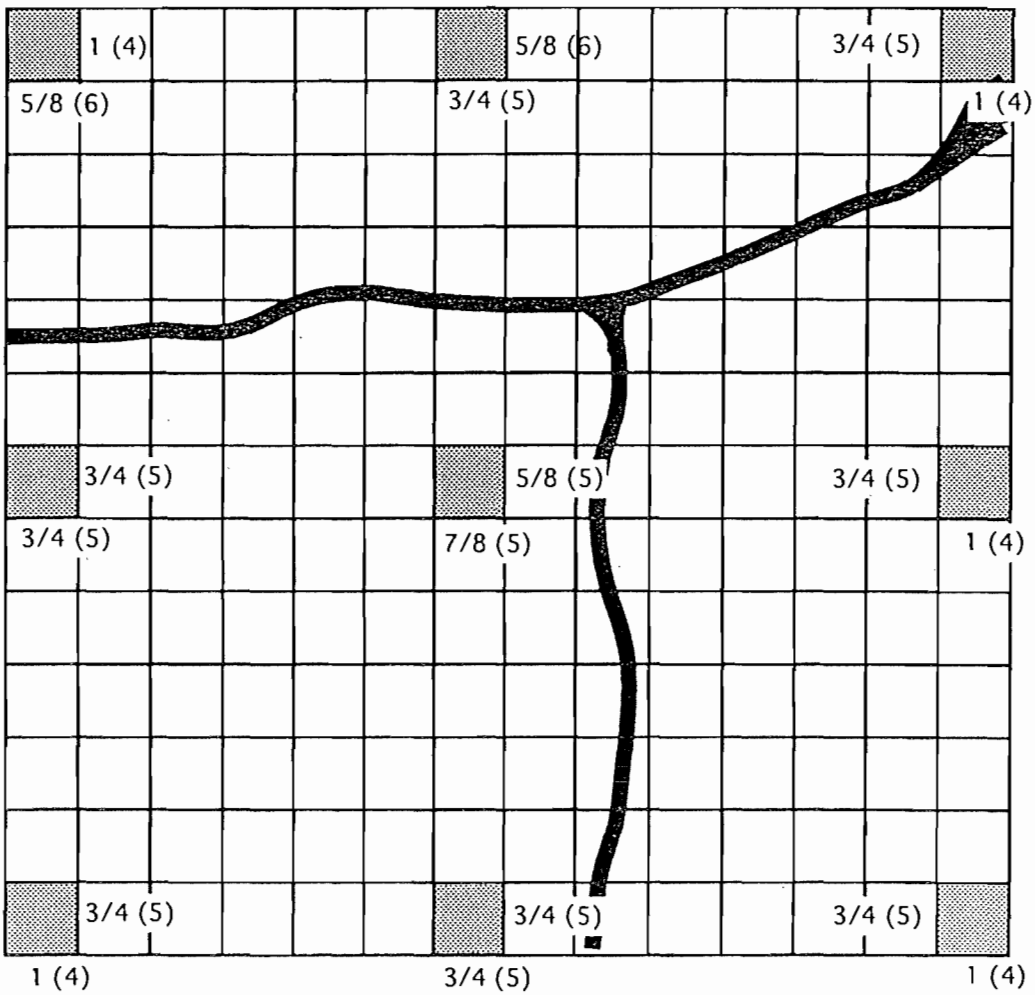

Figure 3.9
Resolution Measured Directly on Image and Computed from Pixel Dimensions of Tiles (given as number of pixels per 1/8 inch 3 mm)

Table 3.1 shows that in the horizontal direction there is 1/16 of an inch (1.6 mm) resolution. This is evident by the minimum pixel values in the 1/16 row that are within a pixel value of the 7/8 row. This is the favorable direction for a camera as the CCD sensor usually has more sensor elements along this direction. Note the pixel variation between samples of about two due to sampling uncertainty.

In the vertical direction the resolution is 1/8 inch (3 mm) due to the 1/8 row minimums being within a *pixel value* of the 7/8 row. Note that all of the pixels are

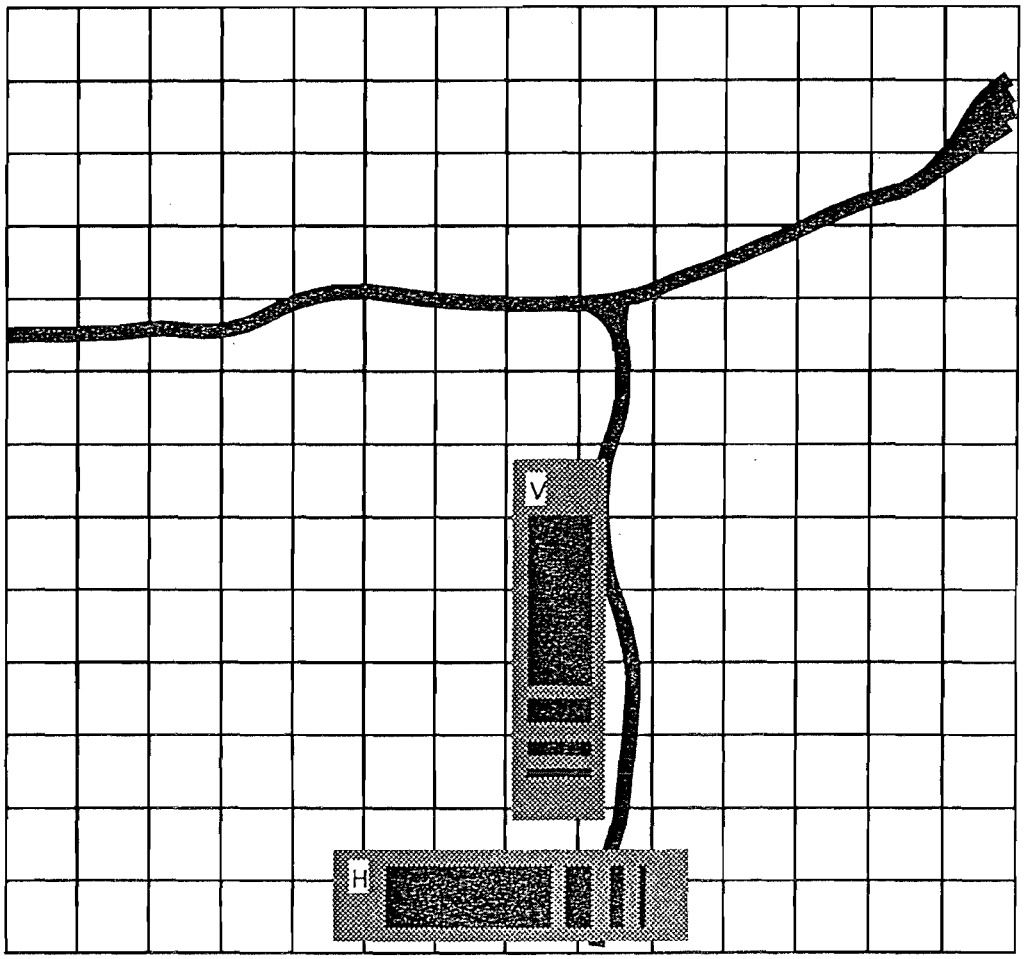

Figure 3.10
Location of Horizontal and Vertical Resolution Test Strips

Horizontal Measurements

1/32	165	157	103	109	153	163	161			
	165	157	101	107	153	163	163			
1/16	167	165	105	63	51	105	159	167		
	167	163	107	59	49	109	157	165		
1/8	163	159	101	59	51	51	47	97	155	161
	163	161	103	57	51	51	47	99	155	161
7/8	163	169	119	63	49	51	53	51	51	53
	165	167	119	59	51	51	53	53	53	51

Table 3.1
Horizontal Pixel Values

Vertical Measurements

1/32	171	169	143	109	127	159	161	163			
	171	169	143	109	127	157	163	163			
1/16	165	165	157	121	65	45	55	115	155	167	
	165	165	157	121	63	43	55	115	155	167	
1/8	169	165	165	163	139	83	43	33	33	33	47
	167	167	167	163	139	83	41	35	33	33	49
7/8	167	167	163	133	69	35	31	31	31	29	31
	167	167	163	133	69	35	33	29	29	29	31

Table 3.2
Vertical Pixel Values

odd values forcing *one pixel value* to actually be considered as two. This could come from a number of hardware sources in the imaging system and is not corrected for testing purposes. Note that even though Fig. 3.9 shows adequate pixel coverage in the vertical direction for 1/16 of an inch (1.6 mm) resolution, the actual resolution is 1/8 of an inch (3 mm). This could be due to the shape and spacing of the individual sensor elements on the CCD employed in the camera and/or the total number of pixels on the CCD in the vertical direction. Some cameras employ half the number of vertical sensor elements that would otherwise constitute the a full picture (approximately 480 pixels) and electronically double the sensor data to create a full-size image. However, the most critical issue is the resolution contained in the digital image in the horizontal and vertical directions for how it has been defined. The spatial resolution in the horizontal direction is 1/16 of an inch (1.6 mm) and the spatial resolution in the vertical direction is 1/8 of an inch (3 mm).

3.3.2 Lighting Quality

Approximate values of ø are computed from 3 crack segments that are similar in appearance in the image. Fig. 3.11 shows approximate widths (in inches) and values of ø (W/D) for three similar segments of the test crack. The

width, W was measured with a 1/32 in (.8 mm) unit ruler. The depth, D was measured with a 1/32 in (.8 mm) diameter steel pin by placing the pin vertically into the crack and measuring the penetration.

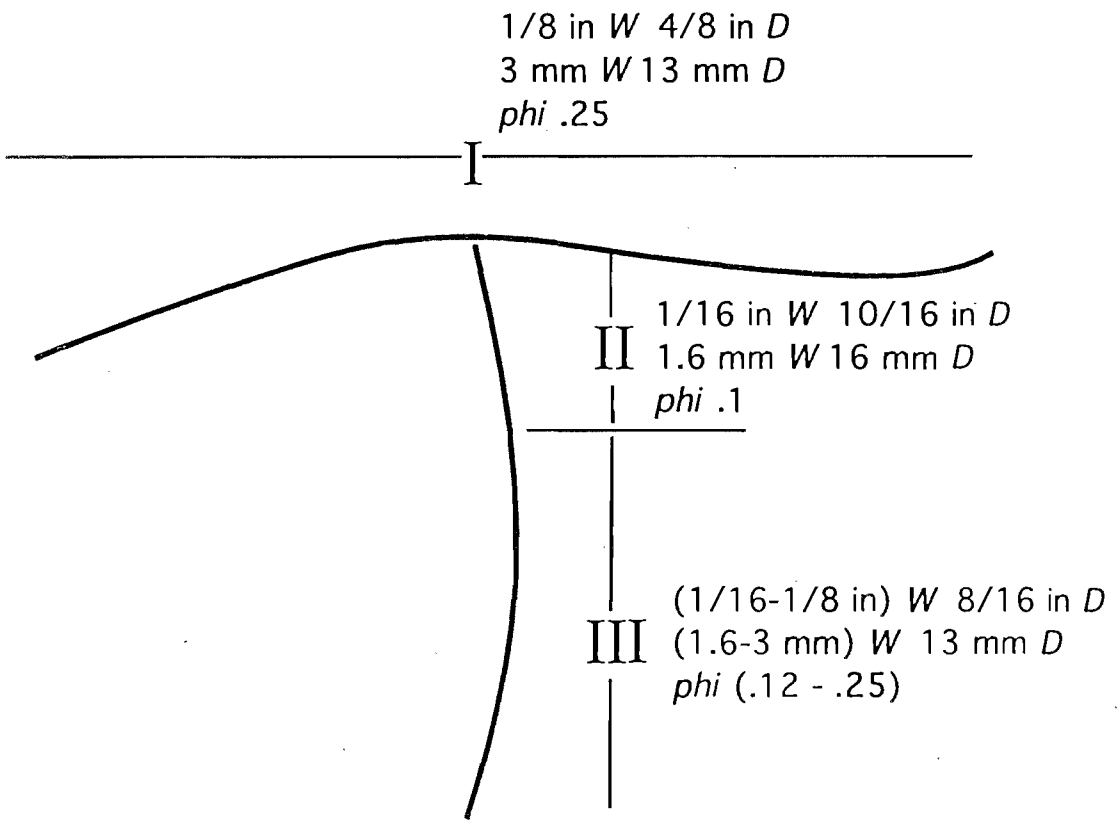

Figure 3.11
Approximate Widths and Values of Ø for Test Crack

Given perfect lighting conditions, we would expect contrast of 92 percent for the top portion of the crack and from 92 to 97 percent for the lower portion of the crack. These percentages are obtained from $(\pi-\phi)/\pi$ as derived in Section 3.1.2. Given background gray level values of about 165 this would produce minimums along the cracks of 152 to 160. The lighting measurements for the top and lower portions of the crack are shown in Figs. 3.12 and 3.13 respectively. Note that the light intensity varies with direction and is therefore not

omnidirectional and varies as much as 70% (measurement of 41.3 foot-candles) for the top segment of the crack at an angle of 40 degrees from the horizon..

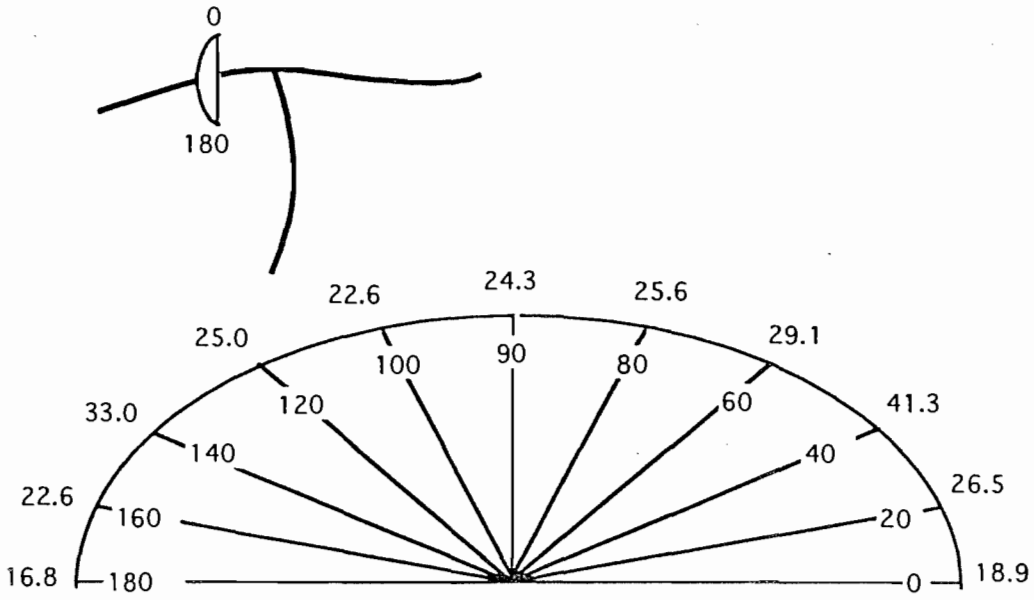

Figure 3.12
Lighting Quality Measured on Top Portion of the Crack
(segment I in Fig. 3.11)

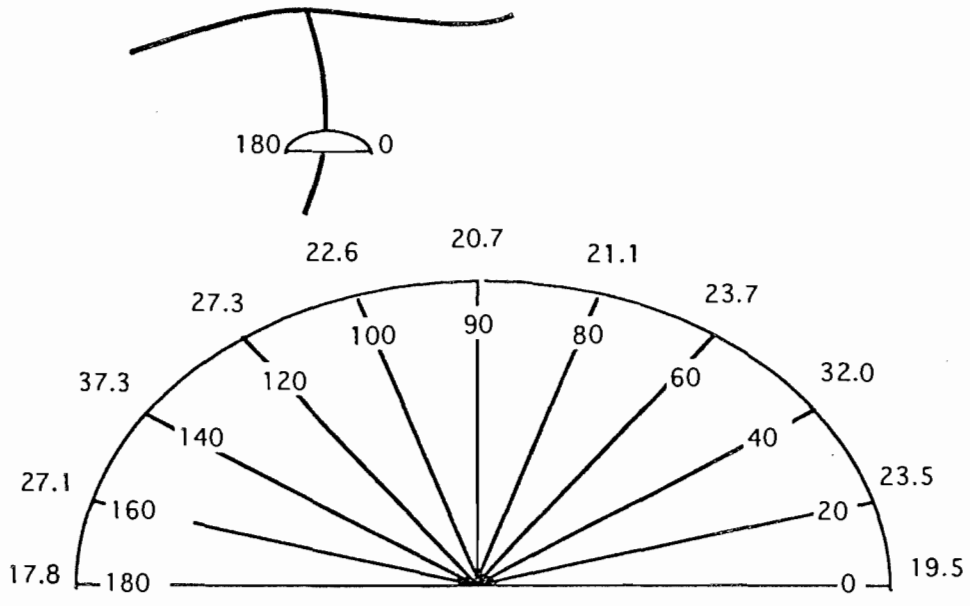

Figure 3.13
Lighting Quality Measured on Bottom Portion of the Crack
(segments II & III in Fig. 3.11)

In order to look at actual minimum pixel values across the crack the tiles on the grid are given reference markers and pixel values are recorded while traversing the crack. The grid and reference markers are shown in Fig. 3.14 and the corresponding pixel values for the traverses are shown in Table 3.3.

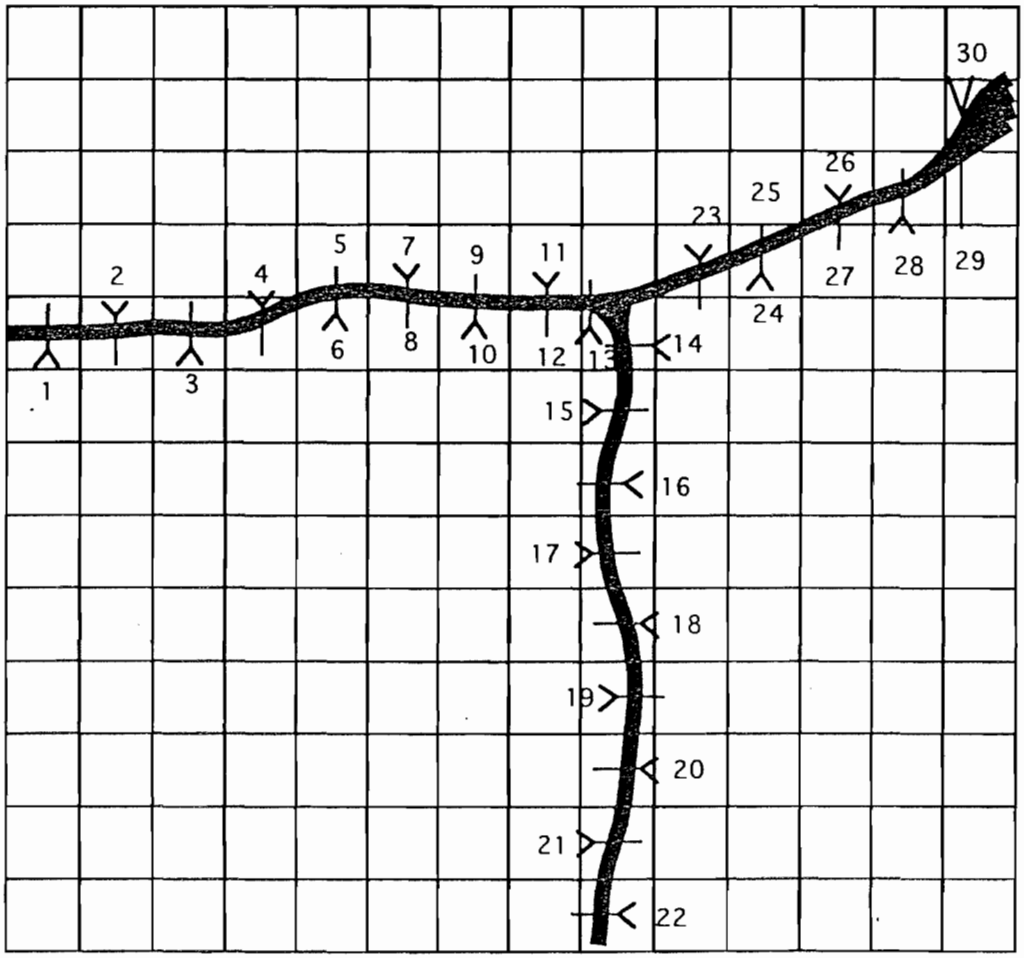

Figure 3.14
Reference Markers for Crack Profiling

From looking at the crack image and cursor location on the monitor while recording the pixel values, it is decided to use a pixel value of 100 or less as the start of a crack in profiling. From this data it looks as though all of the cracks are well represented. Note that the pixel values are much lower at their minimums than expected.

1	151	129	95	61	27	23	25	25	23	31	39	49	79	89	81	87	115	129	129
2	151	139	109	77	73	57	45	83	139	145	119	105	99						
3	169	171	153	107	51	19	19	35	57	67	91	117	131	143	153	165			
4	179	179	167	137	87	83	85	107	147	181	203	203							
6	189	187	153	91	65	61	55	51	53	69	95	115	127	137	141	147			
7	173	177	175	155	157	133	111	85	69	49	33	35	43	51	113	157	179		
10	195	187	137	75	59	53	49	53	81	127	149	159							
11	121	167	159	131	97	89	75	47	39	37	51	105	147	175					
13	197	191	177	179	167	123	71	51	61	67	75	97	129	147	165				
14	171	195	197	189	177	115	73	97	129	135	145	179							
15	189	193	161	125	91	41	81	165	181	187									
16	193	195	175	179	191	179	139	65	59	79	127	177	199						
17	185	201	193	123	69	41	51	127	153	181									
18	179	191	173	79	27	51	55	75	117	133	149	183	185	203					
19	161	167	129	101	87	51	73	151	153	147	151								
20	145	121	119	113	117	115	87	61	95	171	165	137							
21	151	177	149	71	27	21	75	151	177	129	105	131							
22	155	153	145	125	85	69	65	63	83	137	165	149	141						
23	165	167	169	151	89	67	57	105	153	173	189								
24	187	183	187	187	161	107	63	69	91	115	135	161	177	187					
26	193	185	165	131	97	67	51	41	35	35	35	75	129	173	199	195			
28	147	153	147	123	71	57	107	161	171	165	165	177							
30	161	139	113	101	97	79	73	69	69	69	65	57	51	47	39	33	33	29	27

Table 3.3
Profile Values at Reference Markers

There does, however, appear to be sufficient resolution in all of the image for testing algorithm performance. Even the worst profiles shown at row 4, 28 and 14, in Table 3.3 have at least two significantly lower pixel values.

3.3.3 Software Performance

Once the hardware performance is accounted for, algorithm specifics can be addressed. Within the algorithm itself several parameters can be changed. These parameters are:

- the exponent (e) in the moment computation
- an upper offset (uo) whereby gray level values adjacent to the mode during a moment computation are skipped.

Sensitivities of individual parameters are considered as the number of successful crack finds less false positives divided by the total number of cracked tiles. Where the crack occupied two or more tiles in one location only one cracked tile is counted towards the number of cracked tiles as just one tile would successfully locate the crack.

The basic form of the algorithm is the left-hand moment of the distribution relative to the mode (background). A typical shape of the distribution for AC pavements is shown in Fig. 3.15.

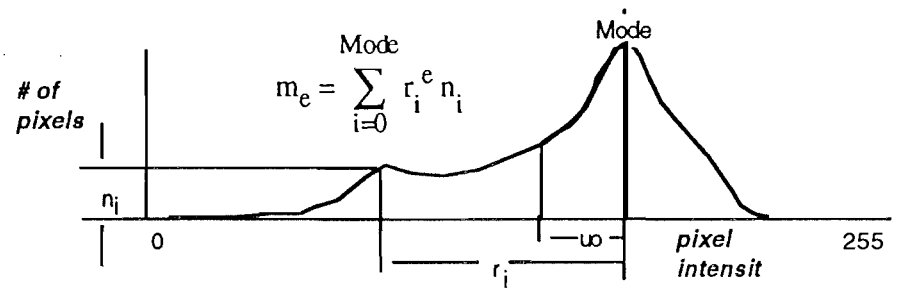

Figure 3.15
Expression for Moment and Typical Shape of Histogram for AC Pavement

An initial implementation of this showed a lack of performance on tall histograms that are produced with Portland Cement Concrete (PCC) pavements. This is due to the fact that crack pixel values are not dispersed as much from the mode as is shown in Fig. 3.16.

In order to increase performance, an upper offset (uo) is used as shown in Fig. 3.15 where data near the mode would be ignored (i.e., the moment computation would begin at an initial r value equal to uo). In order to set this upper offset, the algorithm must be tuned for a particular pavement sample. This is undesirable because excessive attention is required for a continuous operation.

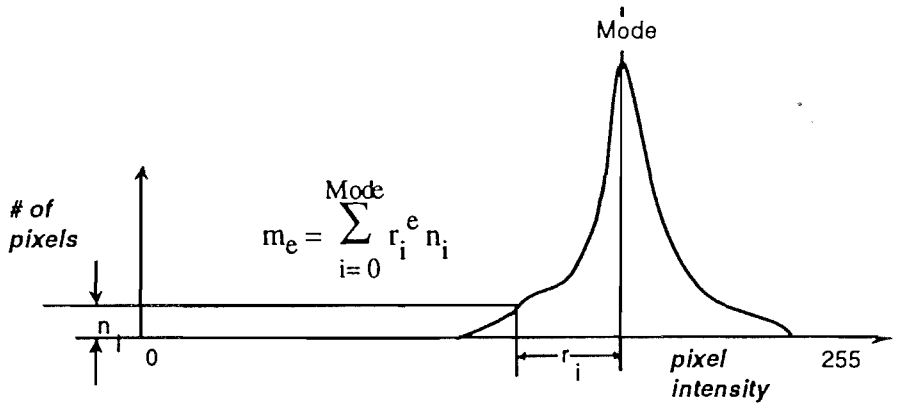

Figure 3.16
Expression for Moment and Typical Shape of Histogram for PCC Pavement

In order to account for different histogram shapes, it is decided that the exponent, e could be a function of r such that values close to the mode receive a relatively small value of e and values close to the end of the distribution receive the full value of the exponent. One method tried is by weighting e based on the cumulative frequency distribution such that e' would be as shown in equation 3.1.

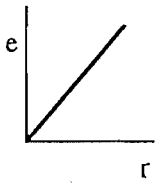

$$e' = e * \frac{\sum_{i=0}^{r} n_i}{\sum_{j=0}^{Mode} n_j} = e * C_r \qquad (3.1)$$

This expression for e would give a somewhat linearly varying exponent depending on the distribution. Another option is tried in order to make the effective exponent, e" in this case, very small near the mode, and remain small until nearly the extreme of the distribution is reached. e" is shown in equation 3.2. The exponential form would seem to be more robust. All three forms of exponents, e, e', and e" are tested.

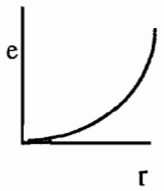

$$e'' = 2e * \left[1-\cos\left(C_r^2\right)\right] \qquad (3.2)$$

The algorithm has three parameters that need to be accounted for in testing, the integer value of the exponent, its weighting, and the upper offset from the mode. The success of each of the 27 possible combinations of the parameters are quantified as the number of correct crack finds less false positives divided by the 22 total possible crack finds.

A 3-way Analysis of Variance (ANOVA) test as explained in Ross (1988) is conducted to obtain optimal algorithm parameters. A description of the ANOVA technique as applied in this test is contained in Appendix C. The data from the tests are shown in Table 3.4. For each combination of variables (A,B,C), two measurements were made. Referring to Table 3.4, for each cell, the left most number represents the number of correct crack finds and the right most number represents the number of false positives. The first observation is on the top of each cell and the second observation is on the bottom. An *observation* is the number of correct crack finds less the number of false positives. Summed results for use in ANOVA computations are shown next to the respective letters that represent specific parameter values. The upper right hand corner of Table 3.4 contains the key for the variables used in the moment equations and the forms of the moment equations themselves.

3.4 Results

The results show that for the crack widths present on the test sample, the image resolution is sufficient in both the vertical and horizontal directions.

266 A_1	304 A_2	331 A_3	A - exp {1,2,3} B - UO {0,30,60} C - e {e,e',e"}	
19 1 13 0	21 0 16 0	21 1 20 1	C_1 107	B_1 288
18 1 13 1	15 1 15 1	16 1 20 1	C_2 91	
09 2 19 1	16 1 17 3	19 1 19 1	C_3 90	
17 1 20 2	21 1 16 1	20 1 21 1	C_1 108	B_2 309
20 1 20 0	16 0 15 0	19 1 20 1	C_2 107	
14 0 15 1	15 1 19 1	18 1 18 1	C_3 94	
19 1 19 1	21 0 21 0	21 1 20 0	C_1 118	B_3 304
13 0 14 2	15 0 19 0	20 1 18 0	C_2 96	
14 3 09 1	18 0 18 0	19 1 18 1	C_3 90	

Table 3.4
Algorithm Test Data
data are recorded in pairs (cf,fp)
two measurements per permutation
cf-correct finds
fp-false positives

Furthermore, the lighting employed was sufficient both in theory and practice to promote sufficient contrast. The best performance of the algorithm was shown to recognize 85% of crack locations correctly and produced 5% false positives. The best performance was obtained with the linear moment equation as indicated in Figure 3.15. The optimal exponent in the moment equation is 3 and the upper offset was chosen to be 5, although it was not found to statistically improve

performance. The upper offsets purpose is to remove expected noise from images with *tall* histograms that may occur during field implementation.

4.1 Hardware Performance

From Figure 3.9, the spatial resolution, following the Nyquist criteria appears to be approximately 1/16 of an inch (1.6 mm). The use of test strips showed that in the horizontal direction, the minimum gray scale values of 1/16 inch (1.6 mm) feature is preserved as the discussion on hardware resolution predicted. That portion of the crack which is vertical (segments II & III) varies in width from 1/16 to 1/8 of an inch (1.6 to 3mm) and is well preserved as is indicated by spatial sampling alone. The test strips in the vertical direction provided only 1/8 inch (3 mm) resolution across the horizontal crack segment in the image which is sufficient as the horizontal part of the crack (segment I) on the test sample is approximately 1/8 inch (3 mm) in width. The lack of resolution in the vertical direction is most likely due to the fact that standard CCD cameras are designed with a resolution bias in the horizontal direction.

4.2 Lighting Performance

Figure 3.11 shows values for ø from .1 to .25 for the cracks in the image. Figure 3.13 shows that the lighting is more intense lower to the horizon (also significantly outside of the projected angle of ø in Fig. 3.8) for both crack directions which for this relatively smooth sample provided an increase in contrast. Another source for this increase in contrast could be from a poor estimate of crack geometry as shown in Fig. 3.11. The actual pixel values across 30 crack locations as shown in Figure 3.14 showed acceptable resolution of crack features for all 30 locations.

Measured hardware and lighting performance in preserving crack features is sufficient for algorithm testing. Furthermore, the criteria for hardware and

lighting performance appear to be sufficient as a bench mark for preserving image features. The vertical resolution in the image is less than expected probably due to camera performance. However, this is compensated for by the wider crack widths for the horizontal segment of the crack.

4.3 Software (Algorithm) Performance

The ANOVA computations from the software performance measurements are shown below in Table 3.5. The meaning of the column headings are explained in Appendix C.

ANOVA TABLE

Source	SS	*v*	SS/ *v*	F	%
A	164.15	2	82.07	9.63	99
B	12.70	2	6.35	.75	
C	70.37	2	35.18	4.13	95
AxB	98.63	4	24.66	2.89	95
AxC	33.96	4	8.49	1.00	
BxC	11.41	4	2.85	.335	
AxBxC	6.26	8	.78	.092	
e	229.96	27	8.52		
T	627.44	53			

Table 3.5
ANOVATable

The statistically significant parameters determined by the ANOVA table are the exponent (A during the test), the weighting of the exponent (C) and the interaction of the exponent (A) and the upper offset (B). Specifically,

- the highest value of the exponent produced statistically better performance
- "no-weighting", e.g., C=1 gave statistically better performance

Therefore, the preferred form of the moment equation is

$$m_e = \sum_{i=0}^{\text{Mode-5}} r_i^3 n_i \qquad (3.3)$$

For the upper offset, uo, 5 is chosen as a nominal value to help performance where very tall histograms may occur; however, it is not presented here as a "tuning parameter". With this moment equation it is expected that given the proper image resolution and lighting quality, about 85% of the crack locations will be found correctly and that approximately 5% of the recognized cracks will be false positives. It is further emphasized that during field experience with this algorithm fundamental changes to the algorithm would be preferred to the introduction of tuning parameters. It is felt that fine tuning would create a lack of robustness and a perceived lack of quality. Although the results here are based on only one structured test using a sample of PCC pavement and preliminary unstructured algorithm testing as shown in Figs. 2.10 through 2.11, the algorithm will have much more opportunities for field testing once it is implemented on the Automated Crack Sealing Machine that is being developed by Caltrans and UC Davis.

CHAPTER 4 CONCLUSIONS AND RECOMMENDATIONS

A technology has been chosen for the development of machine vision for an Automated Crack Sealing Machine (ACSM) that is to work in cooperation with a local laser range finder for crack verification. Additionally, an algorithm has been formulated and tested that will provide for the detection of approximately 85% of crack locations assuming that image resolution and lighting conditions are adequate. If cracks are assumed by the machine vision system to lie in the center of a tile, then a crack lying within a recommended 2 inch (51 mm) tile (see section 2.1, "grid" for details) must be within 1 inch (25 mm) of the actual crack location. The crack sensing requirements dictate that crack starting location is the most important feature for a given crack segment, however the algorithm as formulated and implemented in the C programming language in Appendix B provides direction information for each crack location which could further be used for path planning or the rejection of noise in a post processing stage of image processing if necessary.

Although theoretical criteria set for hardware and lighting performance to support feature recognition through software is more than adequate for system performance, care must be taken to measure hardware and lighting performance for different hardware configurations.

Based on preliminary algorithm testing results, and a conceptual hardware design presented in this thesis, real-time hardware has been purchased. Initial integration of the machine vision hardware has been completed and is being integrated within the ACSM under development by Caltrans and UC Davis. Furthermore, the algorithm developed in this thesis should provide adequate performance in crack detection for the ACSM.

4.1 Conclusions

Requirements for the detection of cracks within the context of an Automated Crack Sealing Machine have been established. Based on a survey of previous work in crack detection and a survey of machine vision technologies that may be applicable to crack detection, an image based machine vision concept has been developed. The conceptual operation of real-time hardware was also developed to provide for the continuous operation that would be required for the ACSM. The real-time hardware includes requirements to synchronize image acquisition with forward vehicle travel and image processing with incremental vehicle travel.

The most significant contribution within the machine vision concept included an algorithm specifically directed towards the detection of pavement cracks that performs in a manner similar to the human visual system. The algorithm includes histogram-based measures of contrast within local areas called *tiles* . The performance of the machine vision system included favorable initial field testing as well as recognizing 85% of possible crack locations on a laboratory specimen of a Portland Cement Concrete (PCC). Also, there were 5% (with respect to possible crack locations) false positives or tiles incorrectly recognized as having cracks. Within the algorithm, parameters such as exponents and forms of moment equations were tested to optimize algorithm performance. A final form of a moment equation that operates on a histogram created from *image tiles* is recommended.

For the task of measuring algorithm performance, machine vision hardware limitations and lighting quality were considered in their effects on contrast at crack locations. The hardware limitations were hypothesized with respect to the camera and digitizer's ability to preserve contrast in the image through the digitization process. Previous research in lighting techniques for

pavement inspection and assumptions regarding crack geometry were used to characterize lighting contribution to image contrast at crack locations (El-Korchi and Wittels 1990, 1991).

Machine vision and/or hardware limitations were overestimated as the measured crack geometry provided more contrast than could be predicted. Adequate contrast was available, however, for the testing of algorithm performance. The algorithm did present limitations. Strings of dark features such as oil spots were incorrectly recognized as cracks as shown in Fig. 2.12. This particular limitation should be resolved with the use of a local range sensor under parallel development.

4.2 Recommendations

Knowing the limits of algorithm performance would prevent the allocation of the ACSM to job sites where it is not likely to perform. While these cases may be few, their occurrence would be prominent in the mind of a maintenance crew and may discourage the use of the ACSM. As a first step, the limits of algorithm performance should be tested for limiting levels of contrast. In other words, algorithm performance should be correlated to levels of image contrast. As a first step, a minimum percentage of correctly recognized crack locations and a maximum percentage (with respect to actual crack locations) of false positives needs to be established. This could be accomplished by simulating path planning results for different crack recognition outcomes.

Once the contrast limitations have been defined, a method to predict contrast in an image should be further developed. The components of a prediction method would include as inputs: a description of crack geometry and surrounding surface condition that would predict a uniform lighting's ability to promote contrast, the effects of lighting non-uniformities in improving/degrading

contrast, and measured effects of hardware (camera and digitizer) on digitized image contrast. The output would be an estimated crack profile represented by gray scale values for a given crack geometry, lighting, and machine vision hardware variables such as camera dynamic range and digitizer resolution. The prediction method would likely contain a device for quantifying crack geometry which may also provide a benefit to crack sealing experts who would want to correlate crack sealing performance with crack shape. A method to predict digitized image contrast is also necessary to predict algorithm performance once algorithm performance has been correlated to image contrast.

As a rough estimate of the performance of real-time hardware purchased for integration with the ACSM, testing should be conducted in a similar manner to that presented in this thesis using pavement sections with various reflective properties and surface roughness in order to better estimate field performance. Surface roughness is important as rough surfaces such as those created from chip seals (a coat of asphalt followed by a spreading of aggregate) would cast a lot of shadows offering potentially competing contrast within the image.

A deficiency of the algorithm is that if there are no cracks on the road the processing demand does not change, i.e., each tile is examined for the possibility of a crack. This inhibits the forward speed of the vehicle. If the tiles searched, tile sizes, sampling within tiles, or moment computation could adaptively vary with crack density, the ACSM could proceed more spontaneously, speeding up between sections where there is no apparent cracking. These are software changes and would be the easiest solution from the user's standpoint. Another solution to this allow for known crack patterns for typical maintenance activities (e.g., regularly occurring transverse cracks) to be input by the user. The effects of running the image processing front end (as described in section 2.2) beyond

the processing rate and returning to a slower speed could also be studied as a possible solution.

Another deficiency of the algorithm is that it will be sensitive to noise on the pavement such as oil spots or any "crack-like" object that may not necessarily be a crack. A local laser range finder under parallel development can account for this deficiency by measuring range information at detected crack locations and aborting crack sealing procedures where necessary.

The algorithm as presented can provide eight directions. These directions could be increased in order to improve performance where the algorithm is omitting crack segments that fall in-between the basic eight directions. This could be accomplished by increasing the 5x5 comparison area or by increasing directions within the existing comparison area.

Finally, given the success in implementing this algorithm in initial field tests and laboratory setting, it is recommended to implement the algorithm using real-time hardware on the ACSM. With the moment equation as shown in equation 3.3, it is expected that given the proper image resolution and lighting quality, about 85% of the crack locations will be found correctly and that approximately 5% of the recognized cracks will be false positives.

REFERENCES

Belangie, M. C., and Anderson, D I., P.E. (1985) "Crack Sealing Methods and Materials for Flexible Pavements", Federal Highway Administration HPR Project # FHWA/UT-85/1.

Bomar, L.C., Horne, W.F., Brown, D.R. and Smart, J.L. (1988) "A Method to Determine Deteriorated Areas in Portland Cement Concrete Pavements", NCHRP Project 10-28, Gulf Research.

Bourely, A.J. (1985) "Investigation of a Robotic Egg Candling System", Thesis at the Ingenieur de l"Ecole Polytechnique, Paris, France.

Butler, B.C. Jr. (1989), "Pavement Surface Distress Segmentation Using Real Time Imaging," *Proc. of First ASCE Int. Conf. on Applications of Advanced Technologies in Transportation Engineering.*

Crick, F., and Koch, C. (1990). "Some reflection on visual awareness." *Cold Spring Harbor symposia on quantitative biology*, Vol. 55, Cold Spring Harbor Laboratory Press, Cold Spring Harbor, N.Y., 953-962.

El-Korchi T. and Wittels, N. Visual Appearance of Surface Distress in PCC Pavements: I Crack Luminance. (1990) In Transportation Research Record 1260, TRB, National Research Council, Washington, C.C., pp 74-83.

El-Korchi, T. et al, Lighting Design for Automated Pavement Surface Distress Evaluation (1991) In Transportation Research Record 1311, TRB, National Research Council, Washington, D.C., pp. 144-148.

Fukuhara, T., Terada, K., Nagao, M., Kasahara, A. and Ichihashi, S. (1990) "Automatic Pavement-Distress-Survey System", *Journal of Transportation Engineering*, ASCE, Vol. 116, No. 3, pp. 280-286.

Haas, C. and Hendrickson, C.T. (1990) "A Model of Pavement Surfaces", Dept. of Civil Engineering, Carnegie Mellon University Technical Report #R90-191.

Haas, C. and Hendrickson, H. (1990) "Computer-Based Model of Pavement Surfaces", Transportation Research Record No. 1260.

Haas, C., Shen H. and Haas, R. (1984) "Application of Image Analysis Technology to Automation of Pavement Condition Surveys," *Proc. Int. Transport Congress, Montreal, Quebec, RTAC.*

Haas, C., Shen H. and Haas, R. (1985) "ADDA System 1 (Automated Distress Data Acquisition)", Final Report OJTCRP Project #21156, Ontario Ministry of Transport.

Humplick, F. and McNeil, S. (1988) "Evaluation of Automated Inspection Systems for Pavement Surface Distress", Working Paper, Massachusetts Institute of Technology, Cambridge, MA, January 1988.

Kirschke, K.R. and Velinsky, S.A. (1992) "A Histogram Based Approach for Automated Pavement Crack Sensing", ASCE Journal of Transportation Engineering, Vol 118, No. 5, October 1992, pp 700-710.

Krulewich, D.A. (1992) "Development of a High Resolution Sensing System for Automated Crack Sealing Machinery", Master's Thesis, University of California, Davis, Department of Mechanical, Aeronautical & Materials Engineering, 115 pp.

Mahler, D.L. (1985) "Final Design of Automated Pavement Crack Measurement Instrumentation from a Survey Vehicle", Final Report DTFH 61-86-C-001, Federal Highway Administration.

Mahler, D.S. and Kharoufa, Z.B. (1990) "Image Processing for a Pavement Crack Monitor", Strategic Highway Research Program Final Report SHRP-ID/FR-90-001.

Maser, K., Brademeyer, D. and Littlefield, R. (1988) "Pavement Condition Diagnosis Based on Multisensor Data", Presented at the 67th Annual Transportation Research Board Meeting.

Maser, K.R. and Schott J. (1981), "Automated Visual Imaging for High Speed Inspection of Large Structures", National Science Foundation Final Report.

Ritchie, S.G. (1990) "Digital Image Concepts and Applications in Pavement Management", *Journal of Transportation Engineering*, ASCE, Vol. 116, No. 3, pp. 287-298.

Ritchie, S.G., Kaseko, M. and Bavarian, B. (1991) "Development of an Intelligent System for Automated Pavement Evaluation", Proc. of Transportation Research Board 70th Annual Meeting January 13-17, 1991, Washington, D.C.

Ross, P.J. (1988) "Taguchi Techniques for Quality Engineering, Loss Function, Orthogonal Experiments, Parameter, and Tolerance Design", McGraw-Hill Book Company.

Velinsky, S.A. and Kirschke, K.R. (1991) "Design Considerations for Automated Crack Sealing Machinery", Proc. of Second ASCE Int. Conf. on Applications of Advanced Technologies in Transportation Engineering, Minneapolis, Minnesota, August 18-21, 1991 pp. 76-80.

Wittels, N, El-Korchi, T. (1990) Visual Appearance of Surface Distress in PCC Pavements: II Crack Modeling. In Transportation Research h Record 1260, TRB, National Research Council, Washington, D.C., pp. 84-90.

Appendix A-Caltrans Crack Sealing Criteria

Memorandum

To: ALL DISTRICT DIRECTORS

Attention Deputy District Directors
Maintenance
All Region Managers and
Superintendents

Date: October 11, 1991

File:

From: DEPARTMENT OF TRANSPORTATION
DIVISION OF MAINTENANCE

Subject: Specifications of Crack Filler/Sealer for Both Division of Maintenance and Maintenance Funded Contracts

In cooperation with Division of Maintenance, the Division of New Technology, Materials and Research has developed four specifications to be used for crack filling/sealing operations. These specifications (attached) supersede all previous specifications. They are:

1. Emulsified Crack Filler (cold-applied)
2. Polyester Fiber Asphalt Crack Filler (hot applied)
3. Modified Asphalt Crack Filler (hot applied)
4. Low-modulus Asphalt Crack Sealant.

These new specifications are intended to be used as a guide in purchasing or contract work, as well as a clarification of which material to use in a given situation. The practice of specifying material by company or brand name should be replaced by using these specifications.

There are other products on the market available through various vendors and suppliers. The representatives of these companies may attempt to have you try their products. It is recommended that prior to using these products, a call be made to Headquarters Maintenance and inquire if these materials have previously been tested by others throughout the State. This will assist in eliminating the duplication of testing products unnecessarily.

Choosing the Right Materials

Crack Fillers

Based upon evaluated projects, research indicates that Nos. I, 2, and 3 crack fillers may actually seal most cracks for one to two years. This can fluctuate based upon climatic conditions, the size and type of crack being treated, temperatures and necessary preparation of the cracks, etc., prior to application. Although the crack may lose its sealing capability within one to two years, it normally remains filled for a longer period of time.

Therefore, it is recommended that crack fillers be used when maintenance surface treatments are planned within one year. Normally crack fillers are initially less in terms of cost compared to crack sealants.

Emulsified, Crack Fillers are normally used on smaller cracks on existing asphalt overlayed roads. Their success on P.C.C. cracks have not been proven and are not normally recommended for P.C.C. crack filling.

Polyester Fiber Asphalt Crackfillers (Hot Applied) seem to be an effective filler on existing asphalt roads for large cracks prior to a maintenance surface treatment. Although they have not been used on P.C.C. cracks much at this time, they show signs of potentially being a good crackfiller for P.C.C. cracks prior to overlays.

Modified Asphalt Crack Fillers (Hot Applied) work for both asphalt concrete and P.C.C. cracks when a Maintenance surface treatments has been scheduled within one year.

Low Modulus Asphalt Crack Sealants are recommended for both A.C. and P.C.C. cracks. Evaluated project research indicate that these types of crack sealers last five years plus in most situations. Therefore, this type of sealant is recommended when there is no maintenance surface treatment planned within one year.

Crack Preparation

Cracked pavement allows water and foreign material to enter the structural section and may cause ultimate failure.

Individual cracks 1/4 (one quarter) inch wide or wider and any areas with extensive finer cracking should be repaired before the rainy season to protect the structural section.

Cracks should be cleaned prior to filling or sealing. When moisture is present or suspected, it is recommended a "Hot Lance" (hot compressed air) be used to prepare the crack immediately prior to application of materials.

All cracks should be squeegeed when necessary after application to save materials, prevent road noise, and to prevent bleeding or masking up through future maintenance surface treatments.

Currently, several products are being evaluated by our Translab for crack fillers/sealers on P.C.C. cracks. Until research is completed and specifications are written for crack filler/sealers for P.C.C. pavements, we recommend using Nos. 3 and 4 as per the recommended guidelines in this memo.

Please note that material suppliers shall furnish a Certificate of Compliance conforming to Section 6-1.07 of Department of Transportation Standard Specifications dated January 1988.

Any questions regarding these specifications should be directed to the HM-1 Program Advisor, Ed Delano, at (916) 654-2456 CALNET 464-2456.

D.C. Boyd
JOHN L. ALLISON, Chief
Division of Maintenance

Attachments

cc: EShirley - Translab
RReese
KGriffin - Office Engineer
JReeves - Office Engineer
RSykes - Construction
JBorden - Traffic Operations
BEveritt
RNevis - Materiel Ops.
EBDelano
ADWells
DBoyd

GH:tc

SPECIFICATIONS FOR MODIFIED ASPHALT CRACK FILLER

The crack filler shall be a mixture of paving asphalt and ground rubber or ground rubber and polymer which conforms to the following requirements:

TEST	TEST METHOD	SPECIFICATION
Softening Point	ASTM D-36	180°F minimum
Cone Penetration @77°F	ASTM D-3407	30 dmm minimum
Resilience @77°F	ASTM D-3407	40% minimum
Flow	ASTM D-3407	3 mm maximum

The gradation of the ground rubber shall be such that 100% will pass a No. 8 sieve.

The modified asphalt material shall be furnished premixed in containers with an inside liner of polyethylene. Packaged material shall not exceed 60 lbs in weight. Storage and heating instructions and cautions shall be supplied by the vendor with each shipment.

The material shall be capable of being melted and applied to cracks and joints at temperatures below 400°F. When heated, it shall readily penetrate cracks 1/4 inch wide or larger.

The vendor shall furnish certification that the material complies with the above requirement.

A certificate of compliance conforming with Section 6-1.07 (Certificates of Compliance) of the Department of Transportation Standard Specifications dated July 1988 shall be supplied with each shipment.

SPECIFICATIONS FOR EMULSIFIED CRACK FILLER

The material shall be an emulsified crack filler which is readily handled at ambient temperatures. It must be capable of being stored for periods of up to six months and be formulated to withstand freeze-thaw cycles. The base materials shall remain ductile with aging and provide resiliency under extreme climatic conditions.

The crack filler shall contain no volatile organic compounds which may contribute to air pollution. Specifications are as follows:

PROPERTY	TEST METHOD	REQUIREMENTS
Viscosity @ 77°F (25°C), SFS	ASTM D-244	25-150
Pumping stability	GB method (1)	pass
5-day settlement test, %	ASTM D-244	5.0 max.
Cement mixing test, %	ASTM D-244	2.0 max.
Sieve test, %	ASTM D-244 (MOD) (2)	0.1 max.
Particle charge test	ASTM D-244 (MOD)	positive
Residue, %	ASTM D-244 (MOD) (3)	64 min.
Test of Residue from ASTM D-244		
Viscosity @ 140°F (60°C), cSt	ASTM D-2170	4,500-9,500

NOTES:

1) Pumping stability is determined by charging 450 ml. of emulsion into a one-liter beaker and circulating emulsion through a gear pump (Roper 29 B22621) having 1/4-inch inlet and outlet. The emulsion passes if there is not significant oil separation after circulating ten minutes.

2) Test procedure identical with ASTM D-244 except that distilled water shall be used in place of two percent sodium oleate solution.

3) ASTM D-244 Evaporation Test for percent of residue is modified by heating a 50 gram sample to 300°F (149°C) until foaming ceases, then cooling immediately and calculating results.

SPECIFICATIONS
FOR
POLYESTER FIBER ASPHALT CRACK FILLER

The crack filler shall be a mixture of paving asphalt and polyester fibers which conform to the following requirements:

ASPHALT--Grade AR-4000 as specified in Section 92, "Asphalt," of the Standard Specifications

POLYESTER FIBER:

• Denier	3 to 5
• Length	6 mm ±
• Color	Natural (white)
• Crimps	None
• Tensile Strength	78,000 to 88,000 psi
• Specific Gravity	1.38
• Melt Temperature	478° F to 490° F.
• Elongation at Break	35-38%

The Polyester Fibers shall be thoroughly mixed with the asphalt at the rate of 5± 1/2 percent by weight of the asphalt.

The asphalt and polyester fiber shall be heated and mixed in a jacketed double boiler type melting unit which is equipped with both agitation and recirculating systems. The temperature of the heat transfer oil in the melting unit should not exceed 425° F. when melting the asphalt and polyester fiber sealant. The melting unit must be capable of safely heating the sealant to 400° F. Crack sealant shall be applied while the temperature range of the sealant is between 325° F. and 375° F., and the ambient temperature is between 10° F. and 90° F.

APPLICATION--The crack sealant material shall be applied only after the joints, cracks and adjacent pavement surfaces have been cleaned by air blasting and are dry and free of dirt, vegetation, debris and loose sealant. Old sealant which protrudes above the pavement surface shall be completely removed. Routing will not be required.

Crack sealant material shall be spread with any type nozzle or device approved for use by the Engineer that will place the material within the specified temperature range and to the proper dimensions.

Sealed cracks that reopen or in which the filler material sags below the surrounding pavement shall be resealed.

August 1991

SPECIFICATIONS FOR LOW-MODULUS ASPHALT CRACK SEALANT

The crack sealant shall be a mixture of paving asphalt and polymer which conforms to the following requirements:

TEST	TEST METHOD	SPECIFICATION
Softening Point	ASTM D-36	180°F minimum
Ductility @4°C 1 cm/min.	ASTM D-113	30 cm minimum
Force Ductility @4°C	Utah DOT Method	4 lb. maximum
Flow	ASTM D-3407	3 mm maximum

The material shall be furnished premixed in containers with an inside liner of polyethylene. Packaged material shall not exceed 60 lbs. in weight. Storage and heating instructions and cautions shall be supplied by the vendor with each shipment.

The material shall be capable of being melted and applied to cracks and joints at temperatures below 400°F. When heated, it shall readily penetrate cracks 1/4 inch wide or larger.

The vendor shall furnish certification that the material complies with the above requirement.

A certificate of compliance conforming with Section 6-1.07 (Certificates of Compliance) of the Department of Transportation Standard Specifications dated July 1988 shall be supplied with each shipment.

Appendix B-PC Software Implementation of Algorithm using Matrox Image Processing Board

Compiled with Microsoft C 6.0 Compiler. (Matrox libraries are included on compile line.)

```
/*  crack.c
*       This program implements a crack detection algorithm and
*       requires a matrox mvp image processing board to run.
*       It assumes the board is strapped at (0xd000, 0x160).
*/

#include <conio.h>
#include <math.h>
#include <errno.h>

#define TILE_XDIM 32
#define TILE_YDIM 32
#define X_TILES (int) (500-40)/TILE_XDIM
#define Y_TILES (int) (442-12)/TILE_YDIM
#define X_START 40
#define Y_START 12
#define MODE_MAX 255
#define MODE_MIN 1
#define PARM_MIN MODE_MIN
#define DAT_BF_SZ TILE_XDIM*TILE_YDIM

void ProcRect();
void FindEm();
int MODE[X_TILES][Y_TILES];
double PARAM[X_TILES][Y_TILES];
double HIST[256];
unsigned char DATBUF[DAT_BF_SZ];
int ROW, COL;
int PARM_OFFSET, E;
int A,B,C; /* test conditions */

main()
{
unsigned char ovrcolr[15],ovrcolg[15],ovrcolb[15];
unsigned char transpalr[256],transpalg[256],transpalb[256]; long int cnt;
unsigned int xx,yy;

/* SETUP TEST PARAMETERS */
printf("Enter Experiment Parameters A B C: ");
scanf("%d %d %d",&A, &B, &C);
if(A==1) E=0;
if(A==2) E=2;
if(A==3) E=3;
```

```
if(B==1) PARM_OFFSET=0;
if(B==2) PARM_OFFSET=30;
if(B==3) PARM_OFFSET=60;
printf("A %d B %d C %d\n", A,B,C);

if (im_init(0xD000,0x160) != 1)
{
        printf("MVP not found at (0x%x, 0x%x)\n", 0xd000, 0x160); return 0;
}

/* Delay to allow PLL to sync up    */
for (cnt = 0; cnt < 20000; ++cnt);

for(;;)
{ /* Beginning of infinite loop */
        /* Setup Overlay and Acquire an image for processing */
        for(cnt=0; cnt<=14; cnt++)
        {
                ovrcolr[cnt]=255;
                ovrcolg[cnt]=255;
                ovrcolb[cnt]=255;
        }

        for(cnt=0; cnt<=255; cnt++)
        {
                transpalr[cnt]=cnt;
                transpalg[cnt]=cnt;
                transpalb[cnt]=cnt;
        }

        im_opmode(2,0);
        im_olutlay(1,ovrcolr,ovrcolg,ovrcolb,transpalr,transpalg,transpalb);
im_slut(1,16);

        im_clear(4,0);
        im_clear(5,0);
        im_outpath(0,-1,0,0);
        im_chan(0);
        im_inmode(1);
        im_sync(1,0);
        im_video(1,1);
        for(cnt=0;cnt<=3;cnt++)
                im_snapshot(0);

        /* Setup for reading image */
        im_outpath(0,-1,2,0);
        im_outmode(0);
        im_opmode(0,0);

        /* Find mode and calulate parameters */
```

```
        for(ROW=0;ROW<Y_TILES;ROW++)
                for(COL=0;COL<X_TILES;COL++)
                        ProcRect();

        /* Set up Buffer for Overlay */


        im_opmode(1,2);


        for(ROW=2;ROW<Y_TILES-2;ROW++)
                for(COL=2;COL<X_TILES-2;COL++)
                        FindEm();

        im_outmode(1);
        im_opmode(3,0);
        im_outpath(0,-1,2,1);
        printf("Frame Processed, Hit return for next frame\n");
        getchar();

        } /* End of infinite loop */
return 0;
} /* End of Main */

void ProcRect()
{
        unsigned int  a, b;
        int x,y;
        unsigned char pixel;
        double max_num, pix_num, Cr, Cu, Cun, Cud, Em, Cum, Cr2, Diff;

        for(a = 0; a<=TILE_YDIM-1; a++)
                for(b = 0; b<=TILE_XDIM-1; b++)
                {

                        x=COL*TILE_XDIM+b+X_START;
                        y=ROW*TILE_YDIM+a+Y_START;
/*\
 *   This part gets the x,y value in the current frame buffer
 *    "pixel" is the value of the pixel
\*/

pixel=(unsigned char) im_pixr(x,y);

/* This part destructively draws grid poinst after data is read */
if (a==0 || b==0 || a==(TILE_YDIM-1) || b==(TILE_XDIM-1))
im_pixw(x,y,0);
if(ROW==2 && COL>1 && COL<X_TILES-2 && (a==0||a==1))
im_pixw(x,y,255);
if(COL==2 && ROW>1 && ROW<Y_TILES-2 && b==0)im_pixw(x,y,255);
```

```
        if(ROW==Y_TILES-3 && COL>1 && COL<X_TILES-2
        && (a==(TILE_YDIM-1)||a==(TILE_YDIM-2)) ) im_pixw(x,y,255);
        if(COL==(X_TILES-3)  &&  ROW>1  &&  ROW<Y_TILES-2&&
b==(TILE_XDIM-1) ) im_pixw(x,y,255);

        DATBUF[(int)a*TILE_YDIM+b]= pixel;

        } /* end of DatBuf fill */

        /*Creates Histogram*/
        for(cnt=0; cnt<=255; cnt++)
                HIST[(int)cnt]=0;
        for(cnt=0; cnt<=TILE_XDIM*TILE_YDIM-1;cnt++)
                HIST[(int)DATBUF[cnt]]++;

        /*Find Mode*/
        max_num=HIST[MODE_MIN];
        MODE[ROW][COL]=MODE_MIN+1;
        for(cnt=MODE_MIN+1; cnt<=MODE_MAX; cnt++)
                if (HIST[cnt]>max_num)
                {
                        MODE[ROW][COL]=cnt;
                        max_num=HIST[cnt];
                }
        /* Check for this foul condition */
        if(MODE[ROW][COL]<=PARM_OFFSET) PARM_OFFSET=0;

        /* Count Number of pixels below and at the mode *\
        pix_num=0;
        for(cnt=MODE[ROW][COL];cnt>=MODE_MIN;cnt--) pix_num+=HIST[cnt];



        /* Compute Parameter */
        PARAM[ROW][COL]=0;
        Cum=0;
         for(cnt=MODE[ROW][COL];cnt>MODE[ROW][COL]-PARM_OFFSET;cnt-
-)
                Cum+=HIST[cnt];
        for(cnt=MODE[ROW][COL] PARM_OFFSET;cnt>=PARM_MIN;cnt--)
        {
                if(C==1)
                {
                        if(E==0)
                        PARAM[ROW][COL]+=HIST[cnt];
                        if(E>0) PARAM[ROW][COL]+=
                        HIST[cnt]*pow((double)MODE[ROW][COL]-cnt, E );

                }
                if( C > 1 )
```

```
        {
                Cum+=HIST[cnt];
                Cr=(double)Cum/pix_num;
                if(C==2)
                {
                        Em=(double)E*Cr;
                        Diff=(double)MODE[ROW][COL]-(double)cnt;
                        if(Diff <= 0) Diff =.0001;
                        PARAM[ROW][COL]+=
                                (double)HIST[cnt]*exp((double)Em*log(Diff));
                        }
                if(C==3)
                {
                        Cr2=Cr*Cr;
                        Cun=(double) ((double)1 - cos(Cr2));
                        Cud=(double) ((double)1 - cos((double)1));
                        Cu=(double) Cun/Cud;
                        Em=(double)E*Cu;
                        Diff=(double)MODE[ROW][COL]-(double)cnt;
                        if(Diff <= 0) Diff = .0001;
                        PARAM[ROW][COL]+=
                                (double)HIST[cnt]*exp((double)Em*log(Diff));
                }
        } /* end of c>1 */

}/* end of for */

} /* end of function */

void Findem()
{
        unsigned int a,b;
        unsigned int x,y;
        int cnt;
        double max_num;
        double c_tiles[12];

/*/ North Comparisons /*/

c_tiles[0]=PARAM[ROW  ][COL-2];
c_tiles[1]=PARAM[ROW  ][COL+2];
c_tiles[2]=PARAM[ROW-1][COL-2];
c_tiles[3]=PARAM[ROW-1][COL+2];
c_tiles[4]=PARAM[ROW-2][COL-2];

c_tiles[5]=PARAM[ROW-2][COL+2];

c_tiles[6]=PARAM[ROW+1][COL-2];

c_tiles[7]=PARAM[ROW+1][COL+2];
```

```
c_tiles[8]=PARAM[ROW+2][COL-2];

c_tiles[9]=PARAM[ROW+2][COL+2];

/* Sort for Largest Value */
max_num=c_tiles[0];
for(cnt=1; cnt<=9; cnt++)
        if (c_tiles[cnt]>max_num)
                max_num=c_tiles[cnt];
/* Compare to North Tiles */
if(PARAM[ROW][COL]>max_num)
if(PARAM[ROW-1][COL]>max_num)
 if(PARAM[ROW-2][COL]>max_num)
if(PARAM[ROW+1][COL]>max_num)
if(PARAM[ROW+2][COL]>max_num)
{ /* Draw Number 1 (N) on screen */
a=12;
b=2;
x=(unsigned int)COL*TILE_XDIM+b+X_START;
y=(unsigned int)ROW*TILE_YDIM+a+Y_START;
im_move(x,y);
im_gtext(1,1,"1");
x=(unsigned int)COL*TILE_XDIM+b+X_START;
y=(unsigned int)(ROW-1)*TILE_YDIM+a+Y_START;
im_move(x,y);
im_gtext(1,1,"1");
x=(unsigned int)COL*TILE_XDIM+b+X_START;
y=(unsigned int)(ROW-2)*TILE_YDIM+a+Y_START;
im_move(x,y);
im_gtext(1,1,"1");
x=(unsigned int)COL*TILE_XDIM+b+X_START;
y=(unsigned int)(ROW+1)*TILE_YDIM+a+Y_START;
im_move(x,y);
im_gtext(1,1,"1");
x=(unsigned int)COL*TILE_XDIM+b+X_START;
y=(unsigned int)(ROW+2)*TILE_YDIM+a+Y_START;
 im_move(x,y);
im_gtext(1,1,"1");
}


/*/ North-North East Comparisons /*/

c_tiles[0]= PARAM[ROW  ][COL-2];
c_tiles[1]= PARAM[ROW  ][COL+2];
c_tiles[2]= PARAM[ROW-1][COL-2];
c_tiles[3]= PARAM[ROW-1][COL+2];
c_tiles[4]= PARAM[ROW-2][COL-2];
c_tiles[5]= PARAM[ROW+1][COL+1];
c_tiles[6]= PARAM[ROW+1][COL-2];
```

```
c_tiles[7]= PARAM[ROW+1][COL+2];
c_tiles[8]= PARAM[ROW-2][COL-1];
c_tiles[9]= PARAM[ROW-1][COL-1];
c_tiles[10]=PARAM[ROW+2][COL+2];

c_tiles[11]=PARAM[ROW+2][COL+1];

/* Sort for Largest Value */
max_num=c_tiles[0];
for(cnt=1; cnt<=11; cnt++)
        if (c_tiles[cnt]>max_num)
                max_num=c_tiles[cnt];

/* Compare to North-North East Tiles */
if(PARAM[ROW][COL]>max_num)
if(PARAM[ROW-1][COL]>max_num)
if(PARAM[ROW-2][COL+1]>max_num)
if(PARAM[ROW+1][COL]>max_num)
if(PARAM[ROW+2][COL-1]>max_num)
{ /* Draw Number 2 (N_NE) on screen */
        a=12;
        b=10;
        x=(unsigned int)COL*TILE_XDIM+b+X_START;
        y=(unsigned int)ROW*TILE_YDIM+a+Y_START;
        im_move(x,y);
        im_gtext(1,1,"2");
        x=(unsigned int)COL*TILE_XDIM+b+X_START;
        y=(unsigned int)(ROW-1)*TILE_YDIM+a+Y_START;
        im_move(x,y);
        im_gtext(1,1,"2");
        x=(unsigned int)(COL+1)*TILE_XDIM+b+X_START;
        y=(unsigned int)(ROW-2)*TILE_YDIM+a+Y_START;
        im_move(x,y);
        im_gtext(1,1,"2");
        x=(unsigned int)COL*TILE_XDIM+b+X_START;
        y=(unsigned int)(ROW+1)*TILE_YDIM+a+Y_START;
        im_move(x,y);
        im_gtext(1,1,"2");
        x=(unsigned int)(COL-1)*TILE_XDIM+b+X_START;
        y=(unsigned int)(ROW+2)*TILE_YDIM+a+Y_START;
        im_move(x,y);
        im_gtext(1,1,"2");
}

/*/ North East Comparisons /*/

c_tiles[0]= PARAM[ROW  ][COL-2];
c_tiles[1]= PARAM[ROW  ][COL+2];

c_tiles[2]= PARAM[ROW-1][COL-2];
```

```
c_tiles[3]= PARAM[ROW-2][COL  ];

c_tiles[4]= PARAM[ROW-2][COL-2];

c_tiles[5]= PARAM[ROW+1][COL+1];

c_tiles[6]= PARAM[ROW+2][COL  ];

c_tiles[7]= PARAM[ROW+1][COL+2];

c_tiles[8]= PARAM[ROW-2][COL-1];

c_tiles[9]= PARAM[ROW-1][COL-1];

c_tiles[10]=PARAM[ROW+2][COL+2];

c_tiles[11]=PARAM[ROW+2][COL+1];

/* Sort for Largest Value */
max_num=c_tiles[0];
for(cnt=1; cnt<=11; cnt++)
        if (c_tiles[cnt]>max_num)

                max_num=c_tiles[cnt];

/* Compare to North-North East Tiles */
 if(PARAM[ROW][COL]>max_num)
if(PARAM[ROW-1][COL+1]>max_num)
if(PARAM[ROW-2][COL+2]>max_num)
if(PARAM[ROW+1][COL-1]>max_num)
if(PARAM[ROW+2][COL-2]>max_num)
{ /* Draw Number 3 (NE) on screen */
        a=12;
        b=18;
        x=(unsigned int)COL*TILE_XDIM+b+X_START;
        y=(unsigned int)ROW*TILE_YDIM+a+Y_START;
        im_move(x,y);
        im_gtext(1,1,"3");
        x=(unsigned int)(COL+1)*TILE_XDIM+b+X_START;
        y=(unsigned int)(ROW-1)*TILE_YDIM+a+Y_START;
        im_move(x,y);
        im_gtext(1,1,"3");
        x=(unsigned int)(COL+2)*TILE_XDIM+b+X_START;
        y=(unsigned int)(ROW-2)*TILE_YDIM+a+Y_START;
        im_move(x,y);
        im_gtext(1,1,"3");
        x=(unsigned int)(COL-1)*TILE_XDIM+b+X_START;
        y=(unsigned int)(ROW+1)*TILE_YDIM+a+Y_START;
        im_move(x,y);
        im_gtext(1,1,"3");
```

```
        x=(unsigned int)(COL-2)*TILE_XDIM+b+X_START;
        y=(unsigned int)(ROW+2)*TILE_YDIM+a+Y_START;
        im_move(x,y);
        im_gtext(1,1,"3");
}


/*/ North East-East Comparisons /*/

c_tiles[0]= PARAM[ROW-2][COL+1];
c_tiles[1]= PARAM[ROW-2][COL  ];
c_tiles[2]= PARAM[ROW-1][COL-2];

c_tiles[3]= PARAM[ROW+2][COL  ];

c_tiles[4]= PARAM[ROW-2][COL-2];

c_tiles[5]= PARAM[ROW+1][COL+1];

c_tiles[6]= PARAM[ROW+2][COL-1];

c_tiles[7]= PARAM[ROW+1][COL+2];

c_tiles[8]= PARAM[ROW-2][COL-1];

 c_tiles[9]= PARAM[ROW-1][COL-1];

c_tiles[10]=PARAM[ROW+2][COL+2];

 c_tiles[11]=PARAM[ROW+2][COL+1];

/* Sort for Largest Value */
max_num=c_tiles[0];
for(cnt=1; cnt<=11; cnt++)
        if (c_tiles[cnt]>max_num)

                max_num=c_tiles[cnt];

/* Compare to North-North East Tiles */
if(PARAM[ROW][COL]>max_num)
if(PARAM[ROW][COL+1]>max_num)
if(PARAM[ROW-1][COL+2]>max_num)
if(PARAM[ROW][COL-1]>max_num)
if(PARAM[ROW+1][COL-2]>max_num)
{ /* Draw Number 4 (NE_E) on screen */
        a=12;
        b=26;
        x=(unsigned int)COL*TILE_XDIM+b+X_START;
         y=(unsigned int)ROW*TILE_YDIM+a+Y_START;
         im_move(x,y);
        im_gtext(1,1,"3");
```

```
        x=(unsigned int)(COL+1)*TILE_XDIM+b+X_START;
        y=(unsigned int)ROW*TILE_YDIM+a+Y_START;
        im_move(x,y);
        im_gtext(1,1,"3");
        x=(unsigned int)(COL+2)*TILE_XDIM+b+X_START;
        y=(unsigned int)(ROW-1)*TILE_YDIM+a+Y_START;
        im_move(x,y);
        im_gtext(1,1,"3");
        x=(unsigned int)(COL-1)*TILE_XDIM+b+X_START;
        y=(unsigned int)(ROW)*TILE_YDIM+a+Y_START;
        im_move(x,y);
        im_gtext(1,1,"3");
        x=(unsigned int)(COL-2)*TILE_XDIM+b+X_START;
        y=(unsigned int)(ROW+1)*TILE_YDIM+a+Y_START;
        im_move(x,y);
        im_gtext(1,1,"3");
}

/*/ East Comparisons /*/

c_tiles[0]=PARAM[ROW-2][COL  ];
c_tiles[1]=PARAM[ROW+2][COL  ];
c_tiles[2]=PARAM[ROW-2][COL+1];
c_tiles[3]=PARAM[ROW+2][COL+1];
c_tiles[4]=PARAM[ROW-2][COL-1];
c_tiles[5]=PARAM[ROW+2][COL-1];
c_tiles[6]=PARAM[ROW-2][COL+2];
c_tiles[7]=PARAM[ROW+2][COL+2];
c_tiles[8]=PARAM[ROW-2][COL-2];
c_tiles[9]=PARAM[ROW+2][COL-2];

/* Sort for Largest Value */
max_num=c_tiles[0];
for(cnt=1; cnt<=9; cnt++)
        if (c_tiles[cnt]>max_num)
                        max_num=c_tiles[cnt];

/* Compare to East Tiles */
if(PARAM[ROW][COL]>max_num)
if(PARAM[ROW][COL-1]>max_num)
if(PARAM[ROW][COL-2]>max_num)
if(PARAM[ROW][COL+1]>max_num)
if(PARAM[ROW][COL+2]>max_num)
{ /* Draw Number 5 (E) on screen */
        a=24;
        b=2;
        x=(unsigned int)COL*TILE_XDIM+b+X_START;
        y=(unsigned int)ROW*TILE_YDIM+a+Y_START;
        im_move(x,y);
        im_gtext(1,1,"5");
```

```
        x=(unsigned int)(COL-1)*TILE_XDIM+b+X_START;
        y=(unsigned int)ROW*TILE_YDIM+a+Y_START;
        im_move(x,y);
        im_gtext(1,1,"5");
        x=(unsigned int)(COL-2)*TILE_XDIM+b+X_START;
        y=(unsigned int)ROW*TILE_YDIM+a+Y_START;
        im_move(x,y);
        im_gtext(1,1,"5");
        x=(unsigned int)(COL+1)*TILE_XDIM+b+X_START;
        y=(unsigned int)ROW*TILE_YDIM+a+Y_START;
        im_move(x,y);
        im_gtext(1,1,"5");
        x=(unsigned int)(COL+2)*TILE_XDIM+b+X_START;
        y=(unsigned int)ROW*TILE_YDIM+a+Y_START;
        im_move(x,y);
        im_gtext(1,1,"5");
}

/*/ East-South East Comparisons /*/

c_tiles[0]= PARAM[ROW-2][COL  ];
c_tiles[1]= PARAM[ROW+2][COL  ];

c_tiles[2]= PARAM[ROW-1][COL+1];

c_tiles[3]= PARAM[ROW-1][COL+2];

 c_tiles[4]= PARAM[ROW+1][COL-1];

c_tiles[5]= PARAM[ROW+1][COL-2];

c_tiles[6]= PARAM[ROW+2][COL+1];

c_tiles[7]= PARAM[ROW+2][COL-1];

c_tiles[8]= PARAM[ROW+2][COL-2];

c_tiles[9]= PARAM[ROW-2][COL-1];

c_tiles[10]=PARAM[ROW-2][COL+1];

c_tiles[11]=PARAM[ROW-2][COL+2];

/* Sort for Largest Value */
max_num=c_tiles[0];
for(cnt=1; cnt<=11; cnt++)
        if (c_tiles[cnt]>max_num)
                max_num=c_tiles[cnt];

/* Compare to East-South East Tiles */
```

```
if(PARAM[ROW][COL]>max_num)
if(PARAM[ROW][COL+1]>max_num)
if(PARAM[ROW][COL-1]>max_num)
if(PARAM[ROW-1][COL-2]>max_num)
if(PARAM[ROW+1][COL+2]>max_num)
{ /* Draw Number 6 (E_SE) on screen */
        a=24;
        b=10;
        x=(unsigned int)COL*TILE_XDIM+b+X_START;
        y=(unsigned int)ROW*TILE_YDIM+a+Y_START;
        im_move(x,y);
        im_gtext(1,1,"6");
        x=(unsigned int)(COL+1)*TILE_XDIM+b+X_START;
        y=(unsigned int)ROW*TILE_YDIM+a+Y_START;
        im_move(x,y);
        im_gtext(1,1,"6");
        x=(unsigned int)(COL-1)*TILE_XDIM+b+X_START;
        y=(unsigned int)ROW*TILE_YDIM+a+Y_START;
        im_move(x,y);
        im_gtext(1,1,"6");
        x=(unsigned int)(COL-2)*TILE_XDIM+b+X_START;
        y=(unsigned int)(ROW-1)*TILE_YDIM+a+Y_START;
        im_move(x,y);
        im_gtext(1,1,"6");
        x=(unsigned int)(COL+2)*TILE_XDIM+b+X_START;
        y=(unsigned int)(ROW+1)*TILE_YDIM+a+Y_START;
        im_move(x,y);
        im_gtext(1,1,"6");
}

/*/ South East Comparisons /*/

c_tiles[0]= PARAM[ROW  ][COL+2];

c_tiles[1]= PARAM[ROW  ][COL-2];

c_tiles[2]= PARAM[ROW+1][COL-1];

c_tiles[3]= PARAM[ROW+1][COL-2];

c_tiles[4]= PARAM[ROW+2][COL  ];

c_tiles[5]= PARAM[ROW+2][COL-1];

c_tiles[6]= PARAM[ROW+2][COL-2];

c_tiles[7]= PARAM[ROW-1][COL+1];

c_tiles[8]= PARAM[ROW-1][COL+2];
```

```
c_tiles[9]= PARAM[ROW-2][COL  ];

c_tiles[10]=PARAM[ROW-2][COL+1];

c_tiles[11]=PARAM[ROW-2][COL+2];

/* Sort for Largest Value */
max_num=c_tiles[0];
for(cnt=1; cnt<=11; cnt++)
        if (c_tiles[cnt]>max_num)
                max_num=c_tiles[cnt];

/* Compare to South East Tiles */
if(PARAM[ROW][COL]>max_num)
if(PARAM[ROW+1][COL+1]>max_num)
if(PARAM[ROW+2][COL+2]>max_num)
if(PARAM[ROW-1][COL-1]>max_num)
if(PARAM[ROW-2][COL-2]>max_num)
{ /* Draw Number 7 (SE) on screen */
        a=24;
        b=18;
        x=(unsigned int) COL*TILE_XDIM+b+X_START;
         y=(unsigned int) ROW*TILE_YDIM+a+Y_START;
        im_move(x,y);
        im_gtext(1,1,"7");
        x=(unsigned int) (COL+1)*TILE_XDIM+b+X_START;
        y=(unsigned int) (ROW+1)*TILE_YDIM+a+Y_START;
        im_move(x,y);
        im_gtext(1,1,"7");
        x=(unsigned int) (COL+2)*TILE_XDIM+b+X_START;
        y=(unsigned int) (ROW+2)*TILE_YDIM+a+Y_START;
        im_move(x,y);
        im_gtext(1,1,"7");
        x=(unsigned int) (COL-1)*TILE_XDIM+b+X_START;
        y=(unsigned int) (ROW-1)*TILE_YDIM+a+Y_START;
        im_move(x,y);
        im_gtext(1,1,"7");
        x=(unsigned int) (COL-2)*TILE_XDIM+b+X_START;
        y=(unsigned int) (ROW-2)*TILE_YDIM+a+Y_START;
        im_move(x,y);
        im_gtext(1,1,"7");
}


/*/ South East-North Comparisons /*/

c_tiles[0]= PARAM[ROW  ][COL+2];
c_tiles[1]= PARAM[ROW  ][COL-2];
c_tiles[2]= PARAM[ROW+1][COL+2];
c_tiles[3]= PARAM[ROW+1][COL-1];
```

```
c_tiles[4]= PARAM[ROW+1][COL-2];
c_tiles[5]= PARAM[ROW+2][COL-1];
c_tiles[6]= PARAM[ROW+2][COL-2];
c_tiles[7]= PARAM[ROW-1][COL-2];
c_tiles[8]= PARAM[ROW-1][COL+1];

c_tiles[9]= PARAM[ROW-1][COL+2];

c_tiles[10]=PARAM[ROW-2][COL+1];

c_tiles[11]=PARAM[ROW-2][COL+2];

/* Sort for Largest Value */
max_num=c_tiles[0];
for(cnt=1; cnt<=11; cnt++)
        if (c_tiles[cnt]>max_num)
                max_num=c_tiles[cnt];

/* Compare to South-East North Tiles */
if(PARAM[ROW][COL]>max_num)
if(PARAM[ROW-1][COL]>max_num)
if(PARAM[ROW-2][COL-1]>max_num)
if(PARAM[ROW+1][COL]>max_num)
if(PARAM[ROW+2][COL+1]>max_num)
{ /* Draw Number 8 (SE_N) on screen */
        a=24;
        b=26;
        x=(unsigned int) COL*TILE_XDIM+b+X_START;
        y=(unsigned int) ROW*TILE_YDIM+a+Y_START;
        im_move(x,y);
        im_gtext(1,1,"8");
        x=(unsigned int) COL*TILE_XDIM+b+X_START;
        y=(unsigned int) (ROW-1)*TILE_YDIM+a+Y_START;
        im_move(x,y);
        im_gtext(1,1,"8");
        x=(unsigned int) (COL-1)*TILE_XDIM+b+X_START;
        y=(unsigned int) (ROW-2)*TILE_YDIM+a+Y_START;
        im_move(x,y);
        im_gtext(1,1,"8");
        x=(unsigned int) COL*TILE_XDIM+b+X_START;
        y=(unsigned int) (ROW+1)*TILE_YDIM+a+Y_START;
        im_move(x,y);
        im_gtext(1,1,"8");
        x=(unsigned int) (COL+1)*TILE_XDIM+b+X_START;
        y=(unsigned int) (ROW+2)*TILE_YDIM+a+Y_START;
        im_move(x,y);
        im_gtext(1,1,"8");
}

} /* End of Findem Function */
```

Appendix C - ANOVA Methodology Description

Analysis of Variance (ANOVA) is a statistical method used to interpret experimental data. The method was developed by Sir Ronald Fisher in the 1930's as a way to interpret the results from agricultural experiments. ANOVA is a statistically based decision tool for detecting any differences in average performance of groups of items tested. A three-way ANOVA entails three controlled variables in an experiment. For the algorithm testing performed in this thesis there is the exponent variable A, the upper offset variable B, and the moment equation variable C. Since each variable can take on 3 different values, there are 27 different combinations of variables. Two observations were made for each combination creating 54 observations. An observation is considered the number of successful crack finds less the number of false positives. The total variation is accounted for by using the squared sum of the observations, SS.

The total variation, SS_T is equal to the variation from all sources and an additional error source which is represented as

$$SS_T = SS_A + SS_B + SS_C + SS_{AxB} + SS_{AxC} + SS_{BxC} + SS_{AxBxC} + SS_e . \quad (C\text{-}1)$$

The *crossed* terms indicated an interaction of variables. With a three-way experimental layout as shown in Table 3.4, these variations can be methodically obtained. SS_A is represented as

$$SS_A = A_1^2/n_{A_1} + A_2^2/n_{A_2} + A_3^2/n_{A_3} - T^2/N \quad (C\text{-}2)$$

where N is equal to the total number of observations(54), T is the sum of all observations and A_1, for example, is the sum of the observations (crack finds less false positives) in column A_1 in Table 3.4. n is the number of observations in a column (18 in this case). SS_B, SS_C, SS_{AxB}, SS_{AxC}, SS_{BxC}, and SS_{AxBxC} are

found similarly by summing observations in table rows and intersections of rows and columns depending on interacting factors to be accounted for. If the interaction of AxB is sought then the A_1,B_1 entries in Table 3.4 would be summed and squared followed by A_2,B_2 until all of the permutations are satisfied. Additionally, SS_A and SS_B would be subtracted from an expression for AxB similar to the right hand side of equation C-2. SS_T is also equal to the sum of the squares of the individual entries in the table less T^2/N. SS_e, the variation to error sources can be determined by finding the remainder of the total variation left from the known sources. Table 4.1 shows the sources and the variation (SS) for the factors in the experiment. Source T is the total variation which is the sum of all of the variation observed in the experiment.

The next column in Table 4.1 is *v*, the degrees of freedom for a particular source. A degree of freedom represents a fair (independent) comparison that can be made within the data. For the variables A, B, and C, the degrees of freedom are the number of levels for each variable (3 in this case) minus one. The degrees of freedom of the interactions of A, B, and C are simply the product of the individual degrees of freedom. The total degrees of freedom for the experiment is equal to the number of observations minus one (53 in our case). The error degrees of freedom is determined as the remainder of the total degrees of freedom left after the known sources are accounted for.

The fourth column in Table 4.1 contains a parameter, SS/v that is used to obtain an F-statistic. An F-statistic is used in an F-test which is a tool that provides a decision at some confidence level as to whether the variance from a particular source is statistically significant. The F-statistic is the variance of an individual factor (normalized by its degrees of freedom) divided by the variance due to error (also normalized). This statistic, along with the respective degrees of freedom used to obtain it, can be referenced in a table that provides information

regarding the probability that the variance is not due to error alone. Two tables were used, a 99% probability table and a 95% probability table. Both tables are contained in Appendix D of Ross (1988).